AMERICAN SOCIETY FOR MICROBIOLOGY | mBio®

Unmasking of CgYor1-Dependent Azole Resistance Mediated by Target of Rapamycin (TOR) and Calcineurin Signaling in *Candida glabrata*

Sonam Kumari,[a] Mohit Kumar,[a,b] ⓘ Brooke D. Esquivel,[c] Mohd Wasi,[d] Ajay Kumar Pandey,[a*] Nitesh Kumar Khandelwal,[a]§ Alok K. Mondal,[d] Theodore C. White,[c] Rajendra Prasad,[b] Naseem A. Gaur[a]

[a]Yeast Biofuel Group, International Centre for Genetic Engineering and Biotechnology, New Delhi, India
[b]Amity Institute of Biotechnology and Integrative Science and Health, Amity University Gurgaon, Haryana, India
[c]School of Biological and Chemical Sciences, University of Missouri at Kansas City, Kansas City, Missouri, USA
[d]School of Life Sciences, Jawaharlal Nehru University, New Delhi, India

ABSTRACT In this study, 18 predicted membrane-localized ABC transporters of *Candida glabrata* were deleted individually to create a minilibrary of knockouts (KO). The transporter KOs were analyzed for their susceptibility toward antimycotic drugs. Although Cg*YOR1* has previously been reported to be upregulated in various azole-resistant clinical isolates of *C. glabrata*, deletion of this gene did not change the susceptibility to any of the tested azoles. Additionally, Cg*yor1*Δ showed no change in susceptibility toward oligomycin, which is otherwise a well-known substrate of Yor1 in other yeasts. The role of CgYor1 in azole susceptibility only became evident when the major transporter Cg*CDR1* gene was deleted. However, under nitrogen-depleted conditions, Cg*yor1*Δ demonstrated an azole-susceptible phenotype, independent of CgCdr1. Notably, Cg*yor1*Δ cells also showed increased susceptibility to target of rapamycin (TOR) and calcineurin inhibitors. Moreover, increased phytoceramide levels in Cg*yor1*Δ and the deletions of regulators downstream of TOR and the calcineurin signaling cascade (Cg*ypk1*Δ, Cg*ypk2*Δ, Cg*ckb1*Δ, and Cg*ckb2*Δ) in the Cg*yor1*Δ background and their associated fluconazole (FLC) susceptibility phenotypes confirmed their involvement. Collectively, our findings show that TOR and calcineurin signaling govern CgYor1-mediated azole susceptibility in *C. glabrata*.

IMPORTANCE The increasing incidence of *Candida glabrata* infections in the last 40 years is a serious concern worldwide. These infections are usually associated with intrinsic azole resistance and increasing echinocandin resistance. Efflux pumps, especially ABC transporter upregulation, are one of the prominent mechanisms of azole resistance; however, only a few of them are characterized. In this study, we analyzed the mechanisms of azole resistance due to a multidrug resistance-associated protein (MRP) subfamily ABC transporter, CgYor1. We demonstrate for the first time that CgYor1 does not transport oligomycin but is involved in azole resistance. Under normal growing conditions its function is masked by major transporter CgCdr1; however, under nitrogen-depleted conditions, it displays its azole resistance function independently. Moreover, we propose that the azole susceptibility due to removal of CgYor1 is not due to its transport function but involves modulation of TOR and calcineurin cascades.

KEYWORDS ABC transporters, azole drug resistance, calcineurin, *Candida glabrata*, TOR pathway

The most widespread human fungal pathogens belong to the genus *Candida*. *Candida glabrata* is a commensal fungus in the human microbiota but is also known to cause superficial to serious life-threatening bloodstream infections (1).

Azoles are first-line antifungals that are used to prevent fungal growth by interfering with ergosterol biosynthesis (2). Fluconazole (FLC), the most commonly used azole, targets 14-α-sterol-demethylase (Erg11) and prevents lanosterol conversion to ergosterol (3). The efficacy of the azoles in the treatment of invasive candidiasis is severely hampered by azole resistance that frequently develops in *C. glabrata* (4, 5). To overcome azole resistance in *C. glabrata*, it is first essential to comprehensively understand the mechanisms by which this species confers resistance to the azoles. Canonical mechanisms of azole drug resistance in *C. glabrata* include mutations in the azole target genes, gain of function (GOF) mutations in the transcription factor (TF) gene Cg*PDR1*, overexpression of efflux pump-encoding genes, and mutations in DNA repair pathway genes (5, 6). Unlike in *C. albicans*, substitution mutations in Cg*ERG11* are a less common mechanism of azole resistance in clinical isolates of *C. glabrata*. However, a few mutations in Cg*ERG11*, such as G944A and I166S, have been reported. These Cg*ERG11* mutations exhibit cross-resistance to both azoles and polyenes (7, 8). The TF CgPdr1 is a central player in the azole resistance acquired during antifungal therapy. Notable reports have shown that *C. glabrata* CgPdr1 directly binds to FLC, which results in activation of drug efflux pumps (9, 10). Moreover, GOF mutations in the putative functional domains of the TF CgPdr1 result in upregulated transcription of ABC transporter coding genes Cg*CDR1*, Cg*PDH1*, and Cg*SNQ2* and increased resistance to azoles (5, 11, 12).

Independent studies have established that ABC drug transporters are major contributors to azole resistance in clinical isolates of *C. glabrata*. For instance, resistant clinical isolates of *C. glabrata* show an increased level of Cg*CDR1* transcript and became azole-susceptible upon Cg*CDR1* deletion. Reintroduction of Cg*CDR1* restored the resistance phenotype (13). The expression of Cg*PDH1*, a close homolog of Ca*CDR2*, was also found to be increased in azole-resistant clinical isolates of *C. glabrata* (14). Further study showed that the deletion of Cg*PDH1* in the Cg*cdr1Δ* strain could increase susceptibility to FLC (15). Thus, both Cg*CDR1* and Cg*PDH1* in tandem or independently contribute to azole resistance in *C. glabrata*. A member of the PDR transporter family, CgSnq2 was also shown to contribute to azole resistance (5). A study has shown increased expression of Cg*SNQ2* in two azole-resistant clinical isolates in which Cg*CDR1* or Cg*PDH1* expression remained unchanged (16). In one of these isolates, Cg*SNQ2* was required for the azole-resistant phenotype (17). Similar studies have demonstrated the role of other ABC transporters in azole resistance, e.g., CgAus1, CgYor1, and CgYbt1. CgAus1 protects cells against azole antifungals in the presence of serum (17–19). The transcript levels of Cg*YOR1* and Cg*YBT1* were found to be upregulated in azole-resistant lab mutants as well as in azole-resistant clinical isolates (20). A previous report also suggested the upregulation of Cg*YCF1*, Cg*YBT1*, and Cg*YOR1* in azole-resistant petite isolates (21).

Pathogenic fungi have also evolved a multitude of stress response pathways that enable cells to tolerate azoles. Key regulators of drug-induced stress are target of rapamycin (TOR) kinase, Hsp90, and calcineurin. It has been established that ABC drug transporters impart drug resistance by drug extrusion from the cell, allowing cells to withstand antifungals. Interestingly, a recent study confirmed that hyper-activation of TOR signaling could significantly contribute to azole resistance in the absence of ABC transporter CaCdr6 in *C. albicans* (22). Noteworthy reports also revealed the elegant role of the TOR cascade, the molecular chaperone Hsp90 and its downstream targets, and calcineurin stabilization in enabling cellular stress responses crucial for the emergence and maintenance of drug resistance in *Aspergillus* and *Candida* species (23, 24).

We have recently inventoried 25 ABC proteins in *C. glabrata* to show that 18 ABC proteins are predicted to be membrane-localized and could be drug transporters. The change in transcriptional response to drug exposure highlighted their roles in *C. glabrata* (25). The role of some of the ABC transporters as major azole transporters has been established; however, the existence of a large number of ABC transporter members in the *C. glabrata* genome prompted us to explore their involvement in azole resistance. For this, we created a minilibrary of deletions for all 18 ABC transporter

members in haploid *C. glabrata*. Individual transporter deletions had no consequence upon susceptibility toward tested azoles and other drugs except in the cases of Cg*cdr1*Δ, Cg*snq2*Δ, and Cg*atm1*Δ, where their disruptions increased susceptibility to few tested drugs.

Strikingly, our double deletions of ABC transporter-encoding genes unmasked the contribution of CgYor1 in azole resistance of *C. glabrata*. Notably, the transcript level of Cg*YOR1* was shown to be higher in various resistant clinical isolates (20); however, there was no direct link for this member of the multidrug resistance-associated protein (MRP) family to azole resistance. Our study shows for the first time that oligomycin (OMY), a well-known substrate of Yor1 in *Saccharomyces cerevisiae* and *C. albicans*, is not a substrate of CgYor1. Instead, CgYor1 imparts azole resistance. Additionally, we report that the repression of TOR and calcineurin signaling and change in sphingolipid compositions in Cg*yor1*Δ are directly associated with the azole-susceptible phenotype.

RESULTS

Single deletions of ABC membrane transporters have no impact on cell growth. To construct a minilibrary of 18 ABC membrane transporter knockouts in *C. glabrata*, single gene deletions were created using a fusion PCR-based method employing a dominant selection marker *NAT1* gene as described previously (26, 27). We assessed if removing a transporter from the genome affects the growth kinetics of the resulting mutant. We employed the microtiter plate-based growth assay to record the growth of all constructs (27). The doubling time of 60 min was recorded for most of the mutants belonging to pleotropic drug resistance (PDR), MRP, and adrenoleukodystrophy (ALDp) subfamilies, which were comparable to the wild-type (WT) cells (Fig. S1a and b). However, Cg*atm1*Δ, a member of the multidrug resistance (MDR) subfamily of transporters, displayed slower growth with a doubling time of 80 min and grew as petite colonies. CgAtm1 is predicted to be localized in the mitochondrial membrane and involved in ATP-dependent Fe-S cluster translocation. The deletion of the gene might be linked to perturbation of mitochondrial function, making the cells petite, which was confirmed by the inability of the mutant to grow on yeast extract peptone glycerol (YPG) medium (Fig. S1c).

Except for Cg*cdr1*Δ, Cg*snq2*Δ, and Cg*atm1*Δ, none of the ABC transporter mutants exhibit susceptibility to tested drugs. The ABC transporter mutant library was screened for susceptibility toward different drugs (Table S3). Notably, the susceptibility to tested drugs remained unchanged in ABC transporter deletants belonging to the MRP and ALDp subfamilies. From the PDR subfamily, only Cg*cdr1*Δ and Cg*snq2*Δ manifested increased susceptibility to select drugs. As expected, Cg*cdr1*Δ cells are highly susceptible to antifungals belonging to the categories of azoles, allylamines, and protein synthesis inhibitors, thus confirming its predominant role as a significant multidrug transporter in *C. glabrata* (Fig. 1). Conversely, Cg*snq2*Δ was only susceptible to the DNA damaging agent 4-nitroquinoline N-oxide (4-NQO) and to the metal chelator 1,10-phenanthroline (OP), known substrates for its homolog ScSnq2 in *S. cerevisiae* (28, 29). The deletion of Cg*ATM1* from the MDR subfamily conferred susceptibility only to azoles and echinocandin caspofungin (CSF) and displayed no change concerning other drug exposure (Fig. 1).

Apart from Cg*cdr1*Δ, Cg*snq2*Δ, and Cg*atm1*Δ, all other transporter mutants remained unresponsive to the tested drug exposure, implying that individually, they have no significant role as drug transporters. However, considering the established role of some of the ABC transporters in clinical azole resistance in *C. glabrata*, we posit that their functions probably remain masked by the presence of dominant transporters such as CgCdr1.

The dominant transporter CgCdr1 masks the function of other transporters. ABC transporters share quite a high amino acid sequence homology and domain organization and have overlapping substrate profiles. For example, CgCdr1 shares a sequence identity of 72.49% with CgPdh1 and 48.19% with CgSnq2. This close similarity among ABC members demands more intense analysis to determine the contribution of each
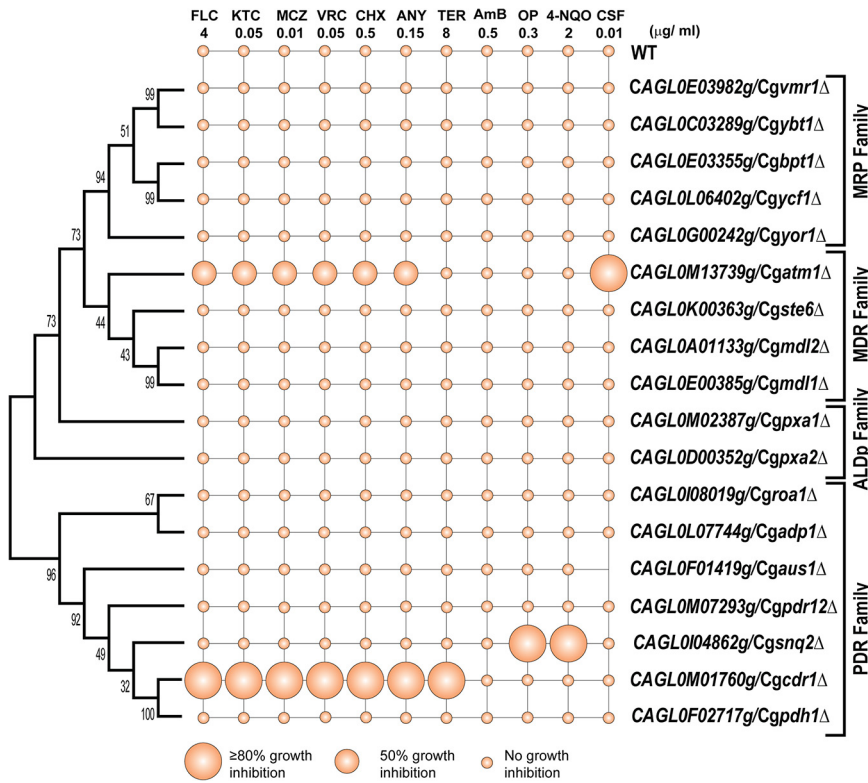
FIG 1 Phenotypic characterization of ABC transporter disruptome. Based on the MIC (MIC$_{80}$), only 3 transporter deletion mutants are susceptible to different antimycotic drugs. A phylogenetic tree was constructed with ClustalW alignment of the complete protein sequence of 18 ABC transporters by MEGA7 with 1,000 bootstrap values.

transporter toward the export of a substrate. The substrate specificity of *S. cerevisiae* ScPdr5, ScSnq2, and ScYor1 are overlapping (30, 31), which strongly suggests redundancy in their transport roles and the possibility of masking of individual function. Notwithstanding the reported dominant impact of CgCdr1 on CgPdh1 and CgSnq2 in *C. glabrata* (5, 15), the fact remains that there are studies pointing to the roles of many other ABC transporters (CgYor1, CgYcf1, and CgYbt1) in clinical azole resistance (18–21). To address this, we constructed double deletions of the transporter genes (Cg*PDH1*, Cg*SNQ2*, Cg*AUS1*, Cg*YCF1*, Cg*YBT1*, and Cg*YOR1*) whose transcripts have been previously reported to be upregulated in drug-resistant clinical isolates of *C. glabrata*. Thus, each of such transporter-encoding genes was deleted in the Cg*cdr1*Δ background (Table S1). These double deletants, Cg*cdr1*Δ/Cg*pdh1*Δ, Cg*cdr1*Δ/Cg*snq2*Δ, Cg*cdr1*Δ/Cg*aus1*Δ, Cg*cdr1*Δ/Cg*yor1*Δ, Cg*cdr1*Δ/Cg*ycf1*Δ, and Cg*cdr1*Δ/Cg*ybt1*Δ, were then subjected to drug susceptibility profiling. The mutants Cg*cdr1*Δ/Cg*snq2*Δ, Cg*cdr1*Δ/Cg*aus1*Δ, Cg*cdr1*Δ/Cg*ycf1*Δ, and Cg*cdr1*Δ/Cg*ybt1*Δ exhibited no change in susceptibility to azoles compared to the Cg*cdr1*Δ strain, implying other cellular roles for these transporters independent from azole response (Fig. 2a). In contrast, Cg*cdr1*Δ/Cg*yor1*Δ and Cg*cdr1*Δ/Cg*pdh1*Δ showed increased susceptibility to azoles compared to Cg*cdr1*Δ (Fig. 2a), which was noticeably absent when these transporters were individually deleted (Table S3). Since the role of CgPdh1 in azole resistance is relatively well established (15), we focused this study on uncovering the role of CgYor1 in azole susceptibility, which remained masked in the presence of CgCdr1.

The noticeably increased azole susceptibility in Cg*cdr1*Δ/Cg*yor1*Δ prompted us to explore if any other transporter could also conceal the influence of CgYor1 on azole susceptibility. To address this, we constructed double KOs in the background of Cg*yor1*Δ, such as Cg*yor1*Δ/Cg*pdh1*Δ, Cg*yor1*Δ/Cg*snq2*Δ, Cg*yor1*Δ/Cg*aus1*Δ, Cg*yor1*Δ/
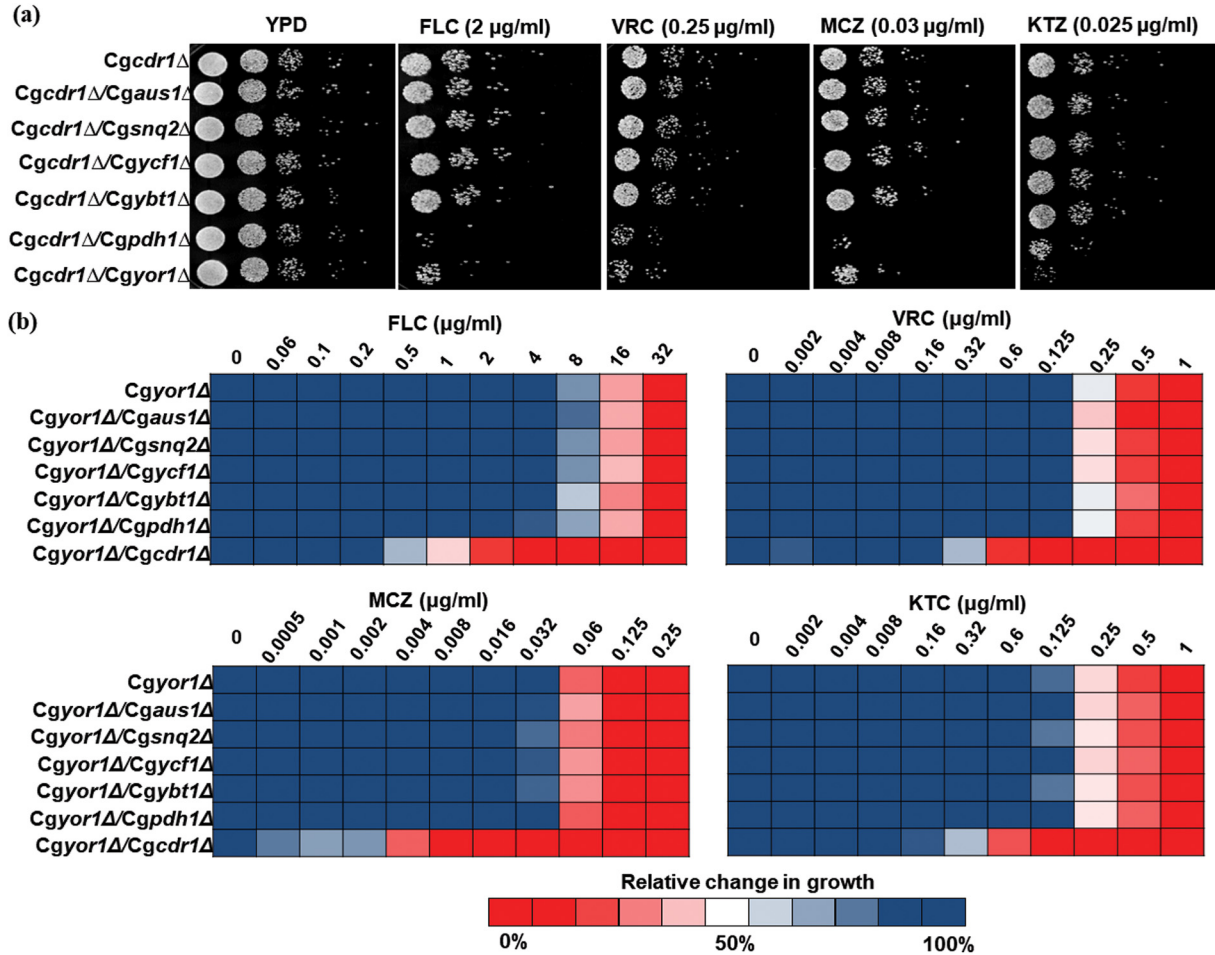
(a)

(b)

FIG 2 Susceptibility of ABC transporter mutants in the background of Cg*cdr1*Δ and Cg*yor1*Δ. Drug susceptibility to FLC, VRC, MCZ, and KTC was determined by (a) spot assays on solid agar media for mutants in the Cg*cdr1*Δ background and (b) broth microdilution in liquid media for mutants in the Cg*yor1*Δ deletion background.

Cg*ycf1*Δ, and Cg*yor1*Δ/Cg*ybt1*Δ. We subjected each of these double KOs to drug susceptibility tests which also included the Cg*yor1*Δ/Cg*cdr1*Δ mutant. Significantly, none of the double KO mutants except Cg*cdr1*Δ/Cg*yor1*Δ could impact azole susceptibility (Fig. 2b). The data suggest that these transporters do not contribute to the masking of CgYor1 function.

CgYOR1 deletion does not impart susceptibility to oligomycin. The topological prediction by TOPOCONS and Scan Prosite indicates that CgYor1 has a basic MRP subfamily topology, which consists of two transmembrane domains (TMDs) and two nucleotide binding domains (NBDs). TMD1 has eight transmembrane helixes (TMHs) followed by NBD1, while TMD2 has six TMHs followed by NBD2 (Fig. 3a). To characterize the localization of this transporter, we expressed the Cg*YOR1* gene in our homologous overexpression system, MSY8, which lacks 7 ABC transporters and has a GOF mutation of TF Cg*PDR1*. We integrated Cg*YOR1* at the hyperactive Cg*CDR1* locus as described earlier (27) and could confirm the overexpression of green fluorescent protein (GFP)-tagged CgYor1 protein by confocal images that showed a proper rimmed appearance at the plasma membrane (Fig. 3b). The properly overexpressed and localized CgYor1-GFP was fully functional, as was evident from its ability to show an elevated level of drug resistance and efflux of R6G, which was similar to the strain overexpressing untagged CgYor1 (Fig. S2a).

In both *S. cerevisiae* and *C. albicans*, Yor1 is known to transport organic anions, especially the macrolide oligomycin (OMY) (32, 33). A cyclic hexadepsipeptide natural
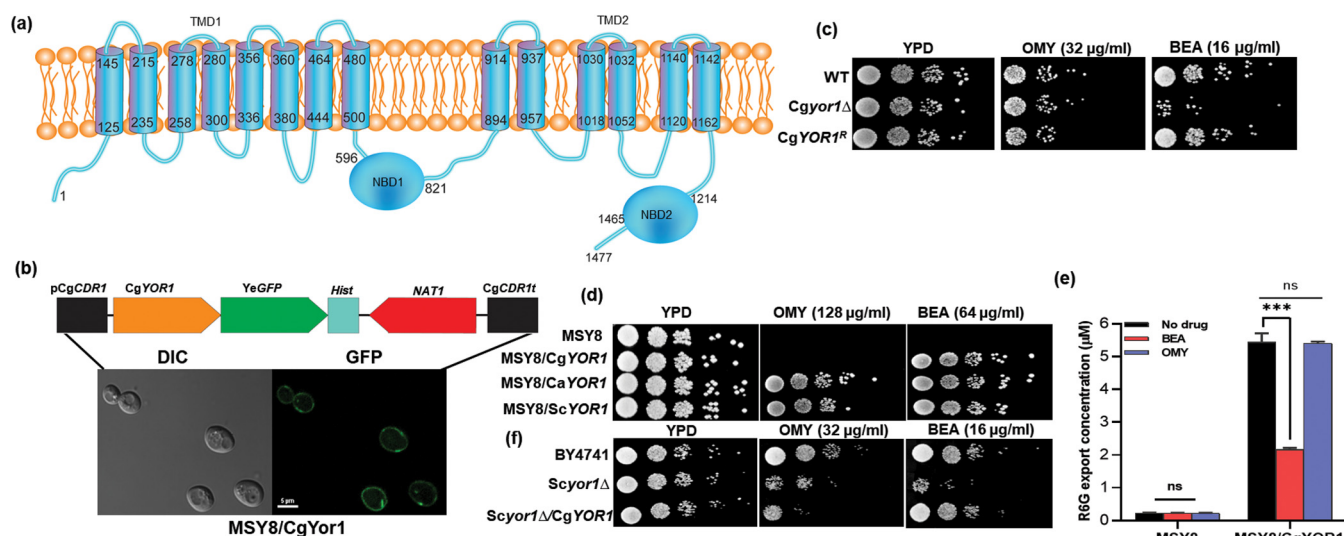
FIG 3 Topology, localization, and substrate specificity of CgYor1. (a) Predicted topology of CgYor1 generated by the softwares TOPOCONS and Scan Prosite results. (b) Localization of CgYor1 by expressing the CgYOR1 gene in the MSY8 strain at the CgCDR1 locus. (c) Spot assay drug susceptibility to OMY and BEA of the CgYOR1 WT, the deletion mutant (Cgyor1Δ), and revertant (CgYOR1R). (d) Spot assay drug susceptibility to OMY and BEA of CgYOR1, CaYOR1, and ScYOR1 overexpressed in heterologous expression system MSY8 at the CgCDR1 locus. (e) Substrate competition; efflux of R6G by the MSY8/CgYOR1 overexpressing strain in the presence of 10× the MIC of BEA or OMY. (f) Complementation of S. cerevisiae Scyor1Δ with CgYOR1 and its susceptibility profile in the presence of OMY and BEA.

product beauvericin (BEA) is another reported substrate of ScYor1 and CaYor1 (34, 35). Surprisingly, while Cgyor1Δ cells showed susceptibility to BEA, the susceptibility to OMY remained unchanged (Fig. 3c). We also tested the probability of enhanced efficacy of FLC and BEA combination treatment after Cgyor1 deletion by employing a dose response matrix. There was greater synergy between FLC and BEA for Cgyor1Δ (fractional inhibitory concentration index [FICI] value, 0.093) than for WT (FICI value, 0.312), but the same was not evident for Cgcdr1Δ cells (FICI value, 1.50), which further supported that BEA is a substrate of CgYor1 (Fig. S2b). However, there was no synergy observed with OMY and FLC in both the mutants Cgyor1Δ and Cgcdr1Δ (data not shown). Further, we tested OMY and BEA susceptibility in the MSY8/CgYOR1 strain overexpressing the CgYor1 transporter. Notably, MSY8/CgYOR1 could not reverse susceptibility to OMY, while it could fully reverse susceptibility to BEA compared to MSY8. Expectedly, MSY8/CaYOR1 and MSY8/ScYOR1 strains reversed susceptibility to both OMY and BEA, suggesting these to be substrates of CaYor1 and ScYor1 (Fig. 3d).

Moreover, substrate competition assays of R6G efflux in the presence of 10× the MIC of either OMY or BEA in the MSY8/CgYOR1 strain further provided credence to our observation. The efflux of R6G by CgYor1 was reduced by half in the presence of BEA but remained unchanged in the presence of OMY (Fig. 3e). To further confirm that OMY is not a substrate of CgYor1, we complemented the Scyor1Δ strain with the CgYOR1 gene and checked its phenotype with respect to OMY and BEA. Notably, the complementation with CgYor1 did not change the Scyor1Δ strain susceptibility to OMY but did reverse the susceptibility to BEA. These results again strengthened our hypothesis that OMY may not be a substrate of CgYor1 (Fig. 3f).

Azoles are not the substrate of CgYor1. Based on the fact that the Cgcdr1Δ/Cgyor1Δ strain is susceptible to azoles, we suspected that azoles could be the substrate of CgYor1. To test this, we measured azole susceptibility in the MSY8/CgYOR1 cells. We noticed the reversal of susceptibility to all the tested azoles in the cells overexpressing CgYor1 (Fig. 4a). To determine whether FLC is the substrate of CgYor1, we performed a time course study of ³H-FLC accumulation in MSY8/CgYOR1 cells as detailed in Materials and Methods. Cells were preloaded with ³H-FLC for 24 h without an energy source, and then 2% glucose was provided as an energy source to activate efflux transporters. Time course analysis of intracellular ³H-FLC levels was performed over 24 h
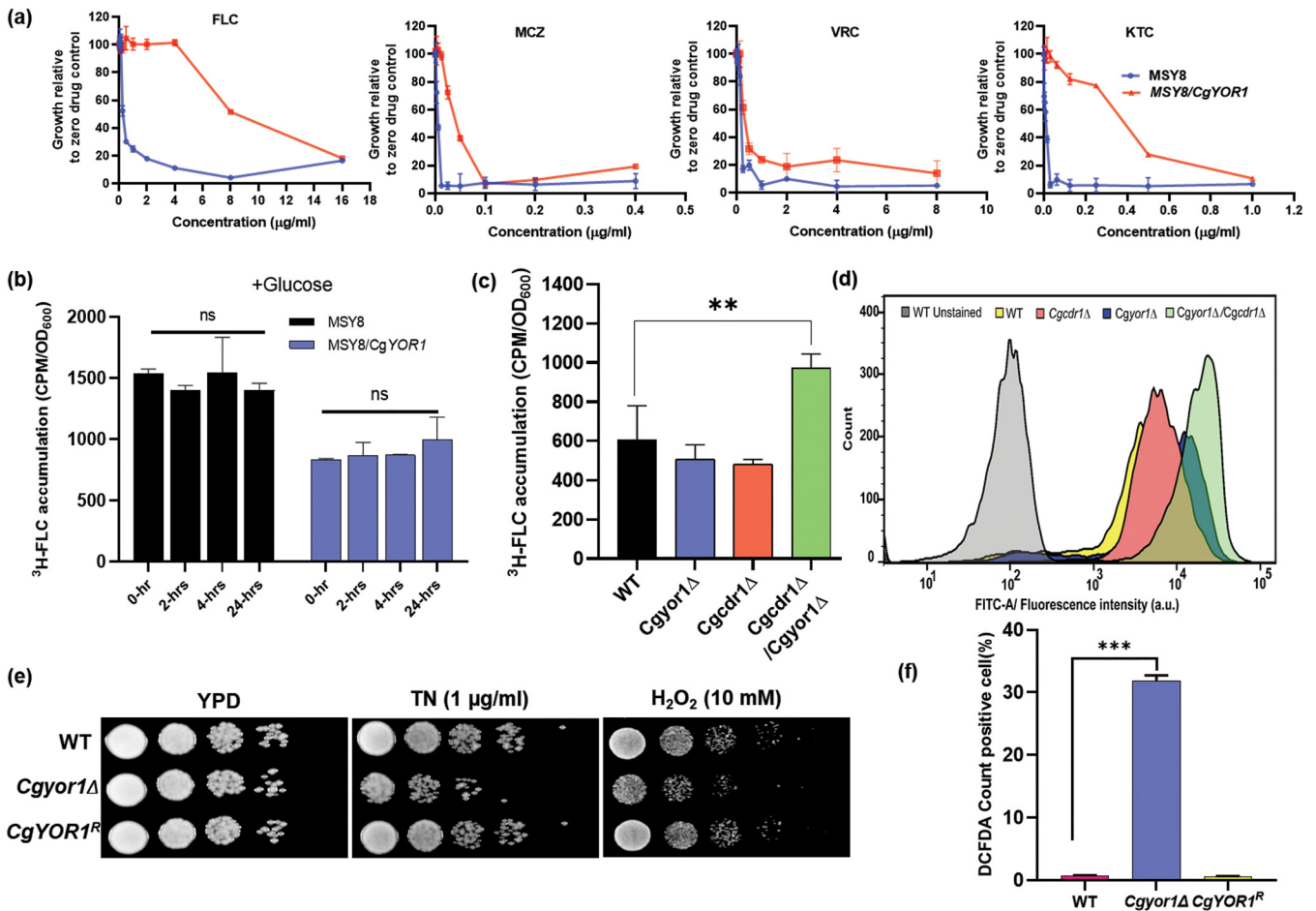
FIG 4 Analysis of factors behind the azole phenotypes of CgYor1. (a) Overexpression of CgYOR1 in MSY8 and phenotypic characterization of azole susceptibility by MIC analysis. (b) ^{3}H-FLC accumulation in MSY8 and MSY8/Cg*YOR1* strains in both the presence and absence of energy. (c) Accumulation of ^{3}H-FLC in the absence of energy to examine the diffusion rate in the Cg*yor1*Δ, Cg*cdr1*Δ, and Cg*cdr1*Δ/Cg*yor1*Δ deletion. (d) R6G accumulation in the strains Cg*yor1*Δ, Cg*cdr1*Δ, and Cg*cdr1*Δ/Cg*yor1*Δ in order to confirm the change in the diffusion of substrates. (e) Cg*yor1*Δ susceptibility to TN and H$_2$O$_2$ by spot analysis displayed increased ER stress and endogenous ROS generation. (f) ROS measurement by FACS analysis using DCFDA in the WT, Cg*yor1*Δ, and Cg*YOR1^R* strains.

upon glucose addition. Intracellular ^{3}H-FLC levels in MSY8/Cg*YOR1* cells at every time point of sample collection showed no reduction, implying that FLC is not transported by CgYor1 (Fig. 4b). To further exclude the possibility of CgYor1 as a transporter of FLC, we also investigated substrate competition with R6G using FLC as the competitive substrate in the MSY8/CgYOR1 strain. We observed that at concentrations of FLC up to 10× MIC, FLC could not compete with R6G efflux, implying that the FLC is not a substrate of CgYor1 (Fig. S3a). Under a similar set of conditions, BEA, which is a known substrate CgYor1, did compete with R6G efflux (Fig. 3e).

Cg*YOR1* deletion in Cg*cdr1*Δ confers enhanced FLC diffusion. The intracellular ^{3}H-FLC accumulation was monitored by incubating the cells with ^{3}H-FLC for 24 h after energy deprivation for 3 h to inhibit the effect of ATP-dependent efflux, as described in Materials and Methods. In the absence of energy, ABC transporters become inactive and the accumulation of ^{3}H-FLC depends on the facilitated diffusion through membrane in fungi (36). We observed reduced ^{3}H-FLC accumulation in MSY8/Cg*YOR*1 cells after the preloading period of 24 h without an energy source compared to the MSY8 strain (Fig. S3b). We speculate that if the overexpression of Cg*YOR1* results in reduced azole accumulation in MSY8/Cg*YOR*1 cells, then the deletion of Cg*YOR1* could increase azole accumulation and susceptibility in Cg*yor1*Δ cells.

We also explored the differences in passive diffusion of FLC, which could explain the increased susceptibility displayed by Cg*cdr1*Δ/Cg*yor1*Δ cells. The observation

obtained from the accumulation analysis of these strains indicates that the double deletion strain Cgcdr1Δ/Cgyor1Δ accumulates a larger amount of ³H-FLC than the WT strain as well as the single deletion strains Cgcdr1Δ and Cgyor1Δ (Fig. 4c). This suggests that the combined deletion of these two membrane transporter genes has dramatically affected the membrane of the strain. The increased accumulation of ³H-FLC after these two gene deletions could be a reason for the enhanced azole susceptibility in the double mutant.

To further confirm that the membrane of the double mutant is compromised and there is a change in the diffusion rate, we performed the accumulation of R6G in these mutant cells. Cells were initially deprived of energy for 3 h and then incubated with R6G for 45 min. The fluorescence-activated cell sorter FACS analyses with these mutants resembled the results with ³H-FLC. The Cgcdr1Δ/Cgyor1Δ mutant displayed a higher accumulation of R6G than the other strains (Fig. 4d). These results suggest a change in membrane diffusion properties in the Cgcdr1Δ/Cgyor1Δ cells may lead to a higher accumulation of FLC inside the cells.

CgYOR1Δ leads to ER stress and enhanced ROS generation. Azoles target ER-localized Erg11 and block the production of ergosterol, which leads to ergosterol depletion from the plasma membrane and the accumulation of toxic sterol intermediates in the cell (37). Independent studies in several pathogenic fungi point to a role of ER stress in influencing antifungal resistance and pathogenesis (38). ER stress has been shown to enhance the effect of azoles and show synergy with the antifungals that lead to a defect in protein folding, Ca2+ homeostasis, and ROS generation (38, 39). Azoles increase reactive oxygen species (ROS) generation in *Candida* and in other fungal species cells, albeit to different magnitudes (40–42).

First, we checked if the targets of azoles are being affected in Cgyor1Δ cells. In this context, the transcript levels of CgERG11, CgERG3, CgERG6, CgERG4, and CgERG2 in Cgyor1Δ cells were assessed by quantitative PCR (qPCR). As evident from Fig. S3d, there was no significant change in *ERG* gene expression. Similarly, spectrometric-based analysis of ergosterol in the mutants also showed no changes in the ergosterol content (Fig. S3c). These data confirmed that Cgyor1Δ cells do not have any major change in the azole target gene and ergosterol content.

The impact of CgYOR1 deletion on ER stress was examined by exposing Cgyor1Δ cells to a well-known ER stress inducer, tunicamycin (TN), which is shown to block the ER enzyme UDP-*N*-acetylglucosamine-1-P transferase required for N-glycosylation in *S. cerevisiae* cells (43). The Cgyor1Δ mutant displayed enhanced susceptibility to TN, which was rescued in CgYOR1^R revertant cells (Fig. 4e). This pointed to an increased ER stress in Cgyor1Δ cells as was also reported in Scyor1Δ cells (44). The deletion of CgYOR1 also conferred increased susceptibility to H_2O_2, indicating defective oxidative stress management (Fig. 4e). Further, we checked the status of endogenous ROS production in the mutant Cgyor1Δ cells. ROS was quantitated by employing an oxidant-sensitive fluorescent probe 2′,7′-dichlorofluorescein diacetate (DCFDA), where its fluorescence intensity is directly proportional to ROS levels (45). By employing FACS analysis, we observed that 30% more Cgyor1Δ cells were taking up DCFDA dye than WT cells and CgYOR1^R revertant cells (Fig. 4f). Together, the observed ER stress and ROS generation in the Cgyor1Δ cells prompted us to explore if these multiple effects can influence the stress-related signaling cascades that could influence azole susceptibility.

Cgyor1Δ mutants display enhanced azole susceptibility under nitrogen depletion conditions. Nitrogen is an essential nutrient for yeast growth, and its availability or scarcity has numerous consequences on gene expression, signaling, and metabolism (46). Nitrogen starvation could have an impact on SNF1/AMP-activated protein kinase (AMPK), cAMP-dependent protein kinase (PKA), and TOR signaling pathways that leads to substantial transcriptomic changes (47). It is established that nitrogen starvation suppresses TOR kinases in several yeasts (48). To assess the impact of nitrogen starvation, we grew the WT strain, the Cgyor1Δ strain, and its revertant CgYOR1^R under both nitrogen-replete (N-replete) and nitrogen-depleted (N-depleted) conditions as detailed in Materials and Methods.
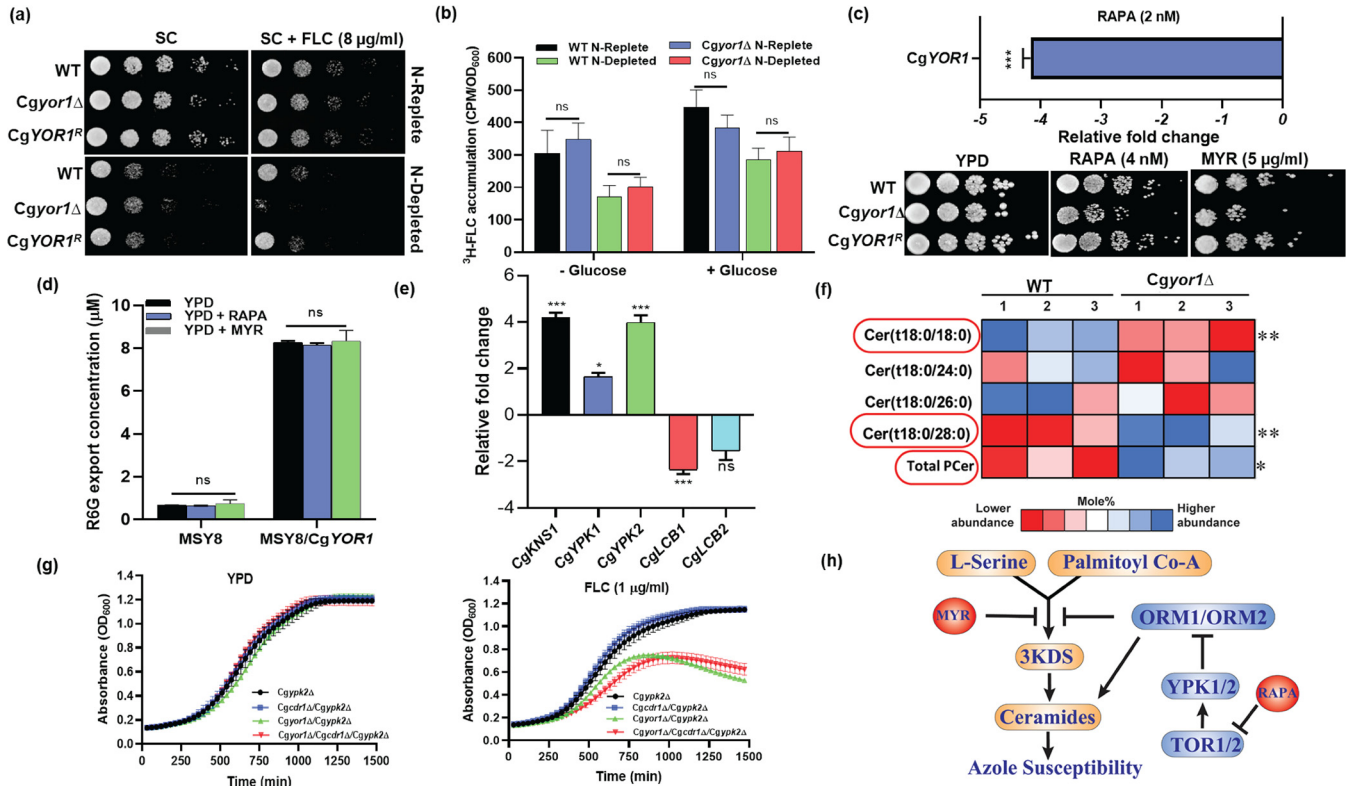
FIG 5 Cg*YOR1* deletion led to suppressed TOR kinase. (a) To assess the impact of nitrogen availability, the WT, Cg*yor1*Δ, and revertant Cg*YOR1*[R] strains were grown under N-replete and N-depleted conditions. Cells were then spotted on SC agar containing FLC. (b) ^{3}H-FLC accumulation under both N-depleted and N-replete conditions in the presence and absence of energy source. (c) Susceptibility of the WT, Cg*yor1*Δ, and Cg*YOR1*[R] strains in RAPA and MYR by spot analysis and transcript-level expression of Cg*YOR1* in the WT strain after transient treatment with RAPA. (d) Substrate competition of RAPA and MYR with R6G. (e) Transcript level expression of TOR kinase downstream effector genes in Cg*yor1*Δ. (f) PCer level comparison in WT and Cg*yor1*Δ. P-Cers with significant differences in abundance are circled in red. 1, 2, and 3 indicate data from triplicate experiments. (g) Growth curves of Cg*ypk2*Δ, Cg*cdr1*Δ/Cg*ypk2*Δ, Cg*yor1*Δ/Cg*ypk2*Δ, and Cg*yor1*Δ/Cg*cdr1*Δ/Cg*ypk2*Δ strains when grown in YPD or YPD +FLC. (h) Schematic displaying the impact of TOR kinase on ceramide level and azole susceptibility.

In agreement with the azole susceptibility data in Fig. 2b, Cg*yor1*Δ single deletion does not alter azole susceptibility compared to the WT strain in N-replete conditions (Fig. 5a). The WT, Cg*Yor1*Δ, and Cg*YOR1*[R] revertant strains were all affected equally by treatment with fluconazole when nitrogen was present. However, after 12 h of growth in N-depleted conditions, the WT, Cg*Yor1*Δ, and Cg*YOR1*[R] revertant strains had reduced growth on agar and grew poorly in liquid media. Addition of FLC further inhibited growth, and FLC susceptibility was more pronounced for all strains under N-depleted conditions (Fig. 5a). This was particularly evident in the Cg*yor1*Δ strain, which showed enhanced susceptibility to FLC under N-depleted conditions. This FLC susceptibility could be rescued to WT levels in Cg*YOR1*[R] cells (Fig. 4a). Noticeably, Cg*cdr1*Δ cells displayed a similar level of susceptibility to FLC under both N-depleted and N-replete conditions (Fig. S4a).

In Cg*yor1*Δ cells grown under N-replete conditions, the transcript of Cg*CDR1* was increased by 2.5-fold (Fig. S4b), which might explain why the Cg*yor1*Δ strain is not susceptible to FLC in the N-replete conditions (Fig. 5a). But under N-depleted conditions, the transcript of Cg*CDR1* was downregulated 4-fold in the Cg*yor1*Δ cells (Fig. S4b). These data imply that CgCdr1 is unable to mask the azole susceptibility phenotype of the Cg*yor1*Δ cells under N-depleted conditions. The change in Cg*CDR1* transcription levels in response to the presence or absence of nitrogen does not affect FLC accumulation into the cells. Under both N-replete and N-depleted conditions, intracellular accumulation of ^{3}H-FLC was very similar in the presence or absence of an energy source (Fig. 5b). Together, these data establish the masking of the CgYor1 function by CgCdr1 under normal growth conditions. The data also support the fact that the azole susceptibility in Cg*yor1*Δ mutant cells may involve the TOR kinases.

Lack of CgYOR1 suppresses TOR signaling. TOR stands for "target of rapamycin" and refers to conserved serine/threonine kinases that control cell growth in response to nutrients (49). In *C. glabrata* two paralogs of TOR kinase (TOR1 and TOR2) exist, which form two structurally and functionally distinct complexes, TOR complex 1 (TORC1) and TOR complex 2 (TORC2) (50). TOR1 is a rapamycin-sensitive kinase that controls cell growth in response to nutrients by promoting anabolic processes such as translation and ribosome biogenesis, while TOR2 is mainly regulated in response to changes in sphingolipid metabolism (51, 52). In *C. albicans* and *S. cerevisiae*, suppression of TOR kinases potentiates the activity of antifungal agents (34).

Involvement of the TOR pathway in the Cg*yor1Δ* phenotype was assayed by comparing the growth of WT, Cg*yor1Δ*, and Cg*YOR1^R* cells in the presence of rapamycin (RAPA), which targets TOR kinase and myriocin (MYR), which acts on the serine-palmitoyltransferase (SPT) complex affecting the sphingolipid homeostasis. We also demonstrated an increased susceptibility of FLC in the Cg*yor1Δ* cells under nitrogen-depleted conditions, which is also an indicator of TOR-suppressed conditions (53, 54). The Cg*yor1Δ* mutant displayed increased susceptibility on both RAPA and MYR, and this susceptibility was rescued in the revertant Cg*YOR1^R* cells (Fig. 5c). Noticeably, the transcript level of Cg*YOR1* was 4-fold downregulated when WT cells were exposed to RAPA (Fig. 5c), while no change was observed in transcripts levels of the other six ABC transporter-encoding genes (Cg*CDR1*, Cg*PDH1*, Cg*SNQ2*, Cg*AUS1*, Cg*YBT1*, and Cg*CYCF1*) (data not shown). To exclude the possibility that CgYor1 could transport RAPA or MYR, we performed a substrate competition efflux assay with R6G in the presence of $10\times$ the MIC of RAPA or MYR in the MSY8/Cg*YOR1* strain. The R6G efflux activity remained unchanged in the presence of excess RAPA and MYR in MSY8/Cg*YOR1* cells, thus ruling out the possibility of RAPA and MYR being substrates of CgYor1 (Fig. 5d).

The involvement of TOR kinase in suppressing the growth of the Cg*yor1Δ* mutant in the presence of FLC was also validated by monitoring transcript levels of the downstream genes (Cg*KNS1*, Cg*YPK1*, Cg*YPK2*, Cg*LCB1*, and Cg*LCB2*) involved in the signaling cascade. *KNS1* is negatively regulated by TOR1 kinase in yeast, and interestingly, the transcript of Cg*KNS1* was upregulated in Cg*yor1Δ* cells, consistent with the suppression of TOR1 in Cg*yor1Δ* mutant cells. Moreover, downregulation of both SPT enzyme-encoding genes, Cg*LCB1* and Cg*LCB2*, was observed in Cg*yor1Δ*, which suggests interference of TOR2 kinase (Fig. 5c and e). This is consistent with MYR susceptibility, which blocks SPT enzymes. TOR1 and TOR2 interact with several downstream effector kinases such as Orm1, Orm2, Ypk1, and Ypk2 in yeast (55). In Cg*yor1Δ*, inactivation of TOR2 kinases activates CgYpk1 and CgYpk2, which can also be seen through their transcript-level expression. The upregulation of Cg*YPK1* and Cg*YPK2* in Cg*yor1Δ* further supports the involvement of TOR kinases (Fig. 5e). Additionally, the deletion of effector kinases (Cg*ckb1Δ*, Cg*ckb2Δ*, Cg*ypk1Δ*, Cg*ypk2Δ*, Cg*cnb1Δ*) in the Cg*yor1Δ* or Cg*yor1Δ*/Cg*cdr1Δ* strain background and their phenotypic analysis in the presence of FLC supported the conclusions.

The susceptibility to MYR and transcript level change in Cg*YPK1* and Cg*YPK2* indicate the involvement of sphingolipids, which are important membrane lipid biomolecules known to regulate various stress-related signaling pathways (56). The sphingolipid profiles of the WT and Cg*yor1Δ* strains were determined by liquid chromatography tandem mass spectrometry (LC-MS/MS)-based analysis. Interestingly, the phytoceramide (PCer) level, which is the most abundant ceramide and can influence azole resistance (57), was significantly increased in the Cg*yor1Δ* mutant (Fig. 5f). A significant increase in Cer(t18:0/28:0) was observed in Cg*yor1Δ* cells, indicating that the increased PCer level could be influencing azole susceptibility. Cer(t18:0/18:0) also displayed significant differences between the WT and Cg*yor1Δ* strains. However, no change was observed in the rest of the major sphingolipids, such as dihydroceramide, α-hydroxyceramides, and others (Table S4).

Ceramide levels can be influenced through TOR2 and regulated by CgYpk1 and CgYpk2. CgYpk1 and CgYpk2 work downstream of TOR2 to regulate the ceramide level

(58). To address the effect of CgYpk1 and CgYpk2 on azole resistance in the Cg*yor1*Δ strain, we have constructed the double mutants Cg*ypk1*Δ/Cg*yor1*Δ and Cg*ypk2*Δ/ Cg*yor1*Δ. Both deletions enhanced the FLC susceptibility of Cg*yor1*Δ; however, the effect of Cg*ypk2*Δ in Cg*yor1*Δ was greater. Importantly, the deletion of Cg*YPK1* and Cg*YPK2* in Cg*cdr1*Δ did not display any further enhanced susceptibility to FLC (Fig. 5g and Fig. S4c). Similarly, deletion strains Cg*orm1*Δ and Cg*orm2*Δ in the Cg*yor1*Δ deletion strain also displayed slightly increased susceptibility, pointing to TOR kinase involvement in the CgYor1 effect on azole susceptibility (Fig. S4c). Together, the data point to the influence of TOR kinases on azole susceptibility by influencing the PCer level through their effector kinases (CgYpk1, CgOrm1, CgOrm2, and especially, CgYpk2) in Cgyor1Δ (Fig. 5h). However, to establish a direct connection between ceramide levels and downstream kinases, further analysis is required.

The absence of CgYor1 suppresses the calcineurin pathway. Calcineurin is a mediator of various stress responses and plays a critical role in mediating drug resistance and virulence in various fungi, including *C. glabrata* (59, 60). Calcineurin, a serine-threonine-specific protein phosphatase, is stabilized by molecular chaperone Hsp90. Hsp90 is phosphorylated by protein kinase CK2, which is a tetramer of four subunits—two activator α-subunits (Cka1 and Cka2) and two regulatory β-subunits (Ckb1 and Ckb2).The KNS1 kinase phosphorylates regulatory subunit CKb2 of CK2, resulting in its activation (61). The active phosphorylated CK2, in turn, phosphorylates Hsp90 and suppresses the calcineurin, which makes cells unable to combat various stresses, including azoles (62, 63). A previous report has indicated that both the regulatory and activation subunits of protein kinase CK2 mutants are involved in azole resistance in *C. albicans* (64). To check whether CK2 is activated in the Cg*cdr1*Δ/Cg*yor1*Δ mutant and has any effect on azole resistance, we constructed the regulatory subunit KO strain in the background of Cg*cdr1*Δ/ Cg*yor1*Δ (Cg*cdr1*Δ/Cg*yor1*Δ/Cg*ckb1*Δ, and Cg*cdr1*Δ/Cg*yor1*Δ/Cg*ckb2*Δ). We observed that Cg*cdr1*Δ/Cg*yor1*Δ harboring any of the regulatory subunit deletions displays reversal of azole susceptibility, implying the effect of protein kinase CK2 on CgYor1-mediated azole susceptibility (Fig. 6a).

The suppression of TOR kinase causes suppression of Hsp90 activity, which destabilizes the protein phosphatase calcineurin, resulting in its deactivation (65, 66). The suppression of CgHsp90 by CK2 activation was also evident with its 2-fold downregulated transcript level in Cg*yor1*Δ cells along with downregulated calcineurin regulatory subunit transcript (Cg*CNB1*) (Fig. 6c). The suppressed calcineurin signaling cascade in the Cg*yor1*Δ mutant was further confirmed when we tested calcineurin inhibitor FK520 susceptibility. We observed that Cg*yor1*Δ mutant cells showed increased susceptibility to FK520. Similarly, we have observed an enhanced susceptibility of the Cg*yor1*Δ mutant toward geldanamycin (GA), an inhibitor of Hsp90. Both FK520 and GA susceptibility are not due to the efflux activity of CgYor1, which was confirmed by their competition with R6G in the MSY8/CgYOR1 strain (Fig. S3e). The susceptibility of the mutant to GA suggests suppressed CgHsp90 in the Cg*yor1*Δ, resulting in unstable calcineurin (Fig. 6b). To further confirm it, we have analyzed the phosphorylation level in CgHog1, which is a mitogen-activated protein kinase (MAPK) of the high osmotic glycerol pathway and is activated under osmotic stress (50). Hsp90 affects activation of Hog1 through its phosphorylation (67). We did not observe CgHog1 phosphorylation in the WT and Cg*yor1*Δ mutant under normal conditions; however, hypo-phosphorylation of CgHog1 became evident in the Cg*yor1*Δ mutant after treatment with salt stress (0.5 M NaCl), which was used to activate CgHog1 phosphorylation (Fig. 6d). The hypo-phosphorylation of CgHog1 in the Cg*yor1*Δ strain confirms less active CgHsp90 in Cg*yor1*Δ mutant cells.

To further investigate the effect of unstable Hsp90 and calcineurin, we constructed a deletion of the regulatory subunit of calcineurin Cg*CNB1*, whose transcript was also downregulated in the Cg*yor1*Δ strain. The Cg*cnb1*Δ in the Cg*yor1*Δ mutant demonstrated a slight increase in susceptibility toward FLC, which indicated that calcineurin is affected in the Cg*yor1*Δ mutant (Fig. S4c). Of note, the zinc finger TF CgCrz1 regulates
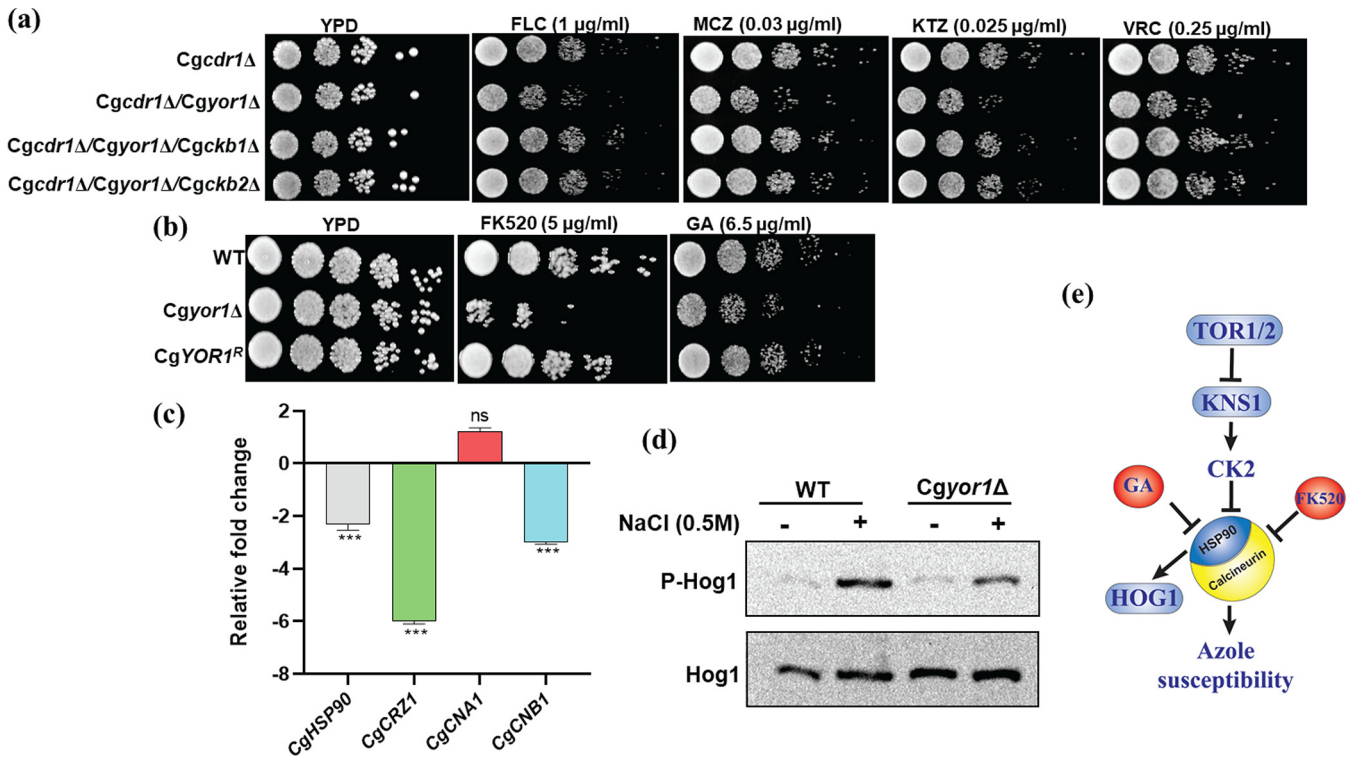
FIG 6 Calcineurin is suppressed in Cg*yor1*Δ. (a) Deletion of the regulatory subunits (CgCkb1 and CgCkb2) of protein kinase CK2 reverses the azole-susceptible phenotype of Cg*cdr1*Δ/Cg*yor1*Δ. (b) Cg*yor1*Δ is susceptible to the calcineurin inhibitor FK520 and Hsp90 inhibitor geldanamycin (GA). (c) Transcript level expression of CgHSP90, calcineurin subunits Cg*CNA*1 and Cg*CNB*1, and the transcription factor-encoding gene CgCRZ1 in Cg*yor1*Δ relative to WT. (d) Phosphorylation of CgHog1 in the presence and absence of salt stress in the WT and Cg*yor1*Δ strains. (e) Pathway displaying the involvement in TOR and calcineurin in azole resistance.

calcineurin function. A 6-fold downregulation of the Cg*CRZ1* transcript in the Cg*yor1*Δ mutant cells further support the link between suppressed calcineurin and azole susceptibility (Fig. 6c). Overall, our results suggest that in the absence of CgYor1, calcineurin protein was suppressed due to hyperactive CK2 and less active Hsp90, thus contributing to azole susceptibility (Fig. 6e).

DISCUSSION

Candida cells harbor a battery of ABC transporters in their genome, and only a few of them have been implicated in clinical drug resistance. The abundance of ABC transporters in *Candida* strongly hints at their multiple roles. This assertion is well supported by several independent observations. For instance, ABC transporters, apart from being drug transporters, are also shown to govern membrane lipid translocation, endocytosis, maintenance of mitochondrial integrity, and many additional virulence traits. (68, 69). ABC transporters such as ScPdr5, CaCdr1, CaCdr2, and CaCdr3 are phospholipid translocators that maintain membrane asymmetry. MRP subfamily transporters (Yor1, Ybt1, Ycf1, Mlt1, and Bpt1) in diverse fungi are involved in the transport of phosphatidylcholine (PC), phosphatidylethanolamine (PE), ions, bile salts, and vacuolar detoxification (70–73). CnAfr1 of *C. neoformans* and AbcB of *Aspergillus fumigatus* are required for pathogenesis (74, 75). Biofilms of *Candida* spp. demonstrate an upregulation of ABC transporters, indicating their potential role in biofilm formation and resistance to antifungals (76–79).

While multiple roles of ABC transporters are becoming increasingly clear, the masking effect due to redundancy and overlap in function, compensatory changes in expression in response to stimulus, the presence of major drug transporters, and other processes may obscure the functional relevance of specific transporters. We addressed this issue using haploid *C. glabrata*, which is one of the most common pathogenic

Candida spp., and created a library of single deletion mutants of all 18 ABC membrane proteins to uncover the function of these transporters. While the phenotypes of our deletion library strains confirm the role of CgCdr1 as a major azole drug transporter in *C. glabrata*, we also discovered that CgYor1 contributes to azole resistance, while it remains masked by CgCdr1. Thus, the role of CgYor1 in azole resistance was only evident in the background of Cg*cdr1*Δ. Notably, besides CgCdr1, no other transporter single or double deletion could unmask the function of CgYor1. We also discovered that unlike the designated function of Yor1 as an OMY transporter in different yeasts, CgYor1 neither impacts susceptibility toward OMY nor transports it. However, as is observed for Yor1 of other yeasts, BEA remains a substrate of CgYor1. The inability of CgYor1 to export OMY is consistent with its failure to complement Sc*yor1*Δ in restoring OMY resistance. The substrate competition studies showing efflux of the test substrate R6G could be competed out by BEA and not by OMY provide further credence to our observation that CgYor1, unlike in other yeasts, does not transport OMY.

A report of an azole-resistant clinical isolate of *C. glabrata* demonstrated a drastic decrease of FLC MIC from 256 μg/mL to as low as 2 μg/mL upon deletion of the TF Cg*PDR1*. However, single deletion of Cg*CDR1* in the same azole-resistant isolate only reduced the FLC MIC to 16 μg/mL. Triple deletions of Cg*CDR1*, Cg*PDH1*, and Cg*SNQ2* resulted in the FLC MIC decreasing to 8 μg/mL (5). These observations strongly suggest that additional undiscovered transporters could contribute to drug resistance in *C. glabrata*. CgYor1 transporter is also part of the regulon of TF CgPdr1 in *C. glabrata*; however, the contribution of CgYor1 in clinical antifungal resistance has not been well defined (10). In this study, we have observed that the azole susceptibility is reversed in the MSY8 strain overexpressing Cg*YOR1*; however, ³H-FLC and efflux data suggest the reversal of azole susceptibility is not linked to FLC transport by CgYor1.

Lipids are a major constituent of plasma membrane and help in maintaining the membrane integrity (80). CgYor1 could be important to maintain membrane lipid homeostasis, which was evident from the altered sphingolipid composition in Cg*yor1*Δ and could be a reason for the increased passive or facilitated diffusion of the ³H-FLC and fluorescent dye R6G in the Cg*cdr1*Δ/Cg*yor1*Δ. The increased intracellular accumulation of FLC could lead to several physiological consequences, as was evident from an increased ROS level and enhanced ER stress in the Cg*yor1*Δ mutant. These changes were suggestive of the involvement of other downstream signaling pathways. For instance, TOR kinases, calcineurin, and their downstream signaling partners are shown to influence azole resistance in *C. albicans* and *S. cerevisiae* (34, 35). Our observations demonstrate that both TOR1 and TOR2 kinases and their downstream signaling partners have important roles in regulating CgYor1-mediated azole resistance. A direct link between CgYor1 and TOR kinases was evident from the fact that the deletion of Cg*YOR1* combined with nitrogen depletion independently suppresses TOR signaling, resulting in increased susceptibility to azoles. Deletion of Cg*CDR1* under nitrogen-depleted and -replete conditions had a similar impact on azole susceptibility, suggesting the independent function of CgYor1 from CgCdr1.

Several studies highlight the signaling role of sphingolipid molecules in multiple cellular processes, including azole resistance (81–83). Sphingolipid long-chain bases (LCBs) are the key intermediates in sphingolipid biosynthesis that include dihydrosphingosine (DHS), phytosphingosine (PHS), and their phosphorylated forms (84). In *C. albicans* azole stress can induce LCB formation where PHS-1-P seems to play an important role in azole resistance by mediating azole accumulation in cells (85). The ceramides are also important as signal molecules that modulate several biochemical and cellular responses to stress stimuli (56, 86). Ceramide and sphingolipid synthesis is coordinated with nutrient availability and cell growth in yeast cells, wherein TOR2 influences LCBs and ceramide synthesis. Ypk1/2 kinases act downstream of TOR2 to activate ceramide synthase activity. We observed that the deletions of these kinases in the background Cg*yor1*Δ resulted in enhanced azole susceptibility, confirming the involvement of these signaling pathways.
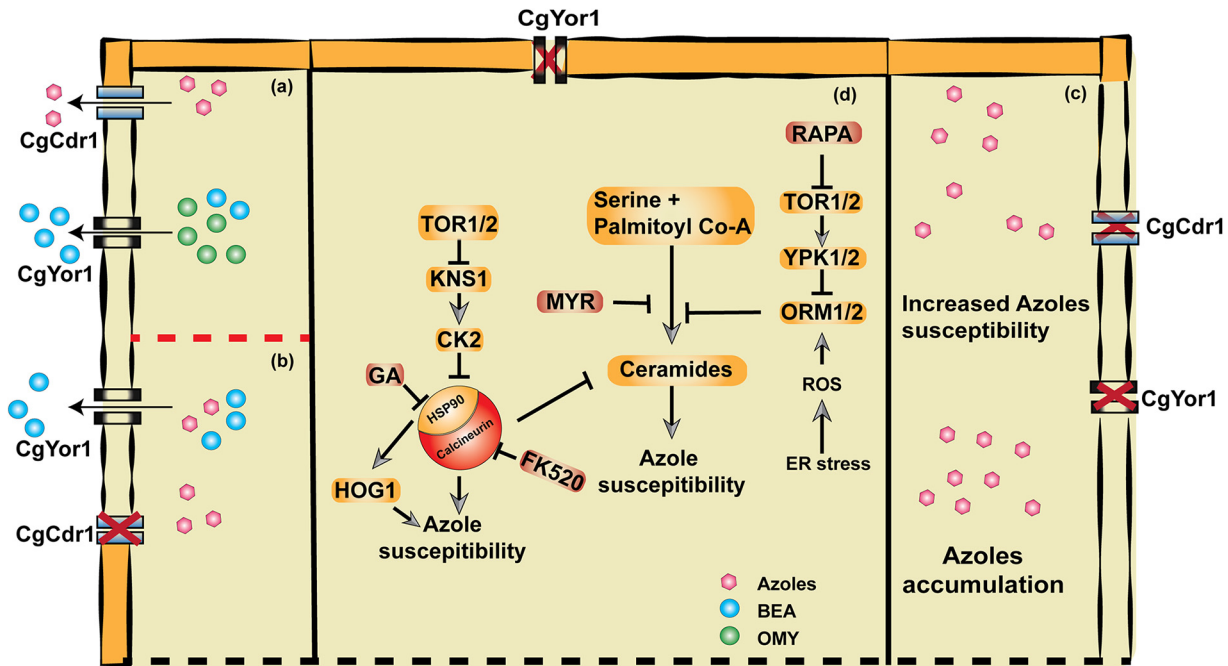
FIG 7 Model to explain the functional characterization of CgYor1. (a) Under normal growth conditions, when WT cells of *C. glabrata* encounter antifungals, CgCdr1 extrudes azoles and CgYor1 extrudes BEA. (b) In the absence of CgCdr1, the cells become susceptible to azoles. (c) In the absence of both the transporters CgCdr1 and CgYor1, enhanced susceptibility with azoles was observed, which could be due to increased accumulation of azoles in the strain. (d) Schematic diagram explaining azole susceptibility in Cg*yor1*Δ involving TOR and calcineurin cascades.

Molecular chaperone Hsp90 interacts with several client proteins to stabilize them or activate them, and through its interactions it generates a profound effect on the cellular stress response (67). The Hsp90 molecule, which is regulated by CK2 kinases, regulates Hog1 by phosphorylation. In the Cg*Yor1*Δ strain, the reduced phosphorylation of CgHog1 is indicative of suppressed CgHsp90 activity. Hsp90 also regulates resistance to both azoles and echinocandins by stabilizing the protein phosphatase calcineurin in *C. albicans* (87, 88). Calcineurin, which is a conserved Ca^{2+}-calmodulin-activated protein phosphatase, has several functions related to calcium-dependent signaling and regulates several important cellular processes in yeasts. The role of the calcineurin pathway in azole resistance and virulence is well established in *C. albicans* and *Candida dubliniensis* (89). The calcineurin and *crz1* mutants in these yeasts show reduced tolerance to azoles and echinocandins (90, 91). We also observed that the Cg*yor1*Δ mutant is susceptible to calcineurin inhibitors. The deletion and phenotypes of CK2 regulatory subunits in the Cg*cdr1*Δ/Cg*yor1*Δ background reverted its azole-susceptible phenotype, which hints at suppressed calcineurin in the mutant.

In conclusion, we are tempted to speculate that the deletion of Cg*YOR*1 results in perturbation of the membrane lipid composition that changes diffusion of FLC, leading to enhanced accumulation of drug and increased susceptibility to azoles. Noticeably, we find that the contribution of CgYor1 to azole susceptibility is independent of the major transporter CgCdr1. However, when CgCdr1 is present, it masks the effects of CgYor1. Importantly, CgYor1 does not transport OMY and FLC but contributes to azole resistance via ROS generation, suppressed TOR, and calcineurin signaling linked to altered sphingolipid homeostasis (Fig. 7). The accurate measurement of membrane composition and organization in CgYor1 cells and how selective CgYor1 deletion triggers the stress pathway are some aspects that remain to be evaluated. Nonetheless, the work highlights that, unlike other homologues, CgYor1 does not function as an OMY exporter in *C. glabrata* cells but contributes exclusively to azole resistance by activating stress signaling pathways.

MATERIALS AND METHODS

Chemicals and strains. Antifungal drugs were of analytical grade and were purchased from Sigma. Yeast strains were maintained in yeast extract peptone dextrose (YPD) medium and in synthetically complete (SC) medium (0.67% yeast nitrogen base, 2% glucose and amino acids), wherever needed. Bacterial cultures were maintained in Luria-Bertani (LB) medium with the final concentration of ampicillin at 100 μg/mL, if needed. Bacterial strain *Escherichia coli* DH5α was used to maintain plasmids. Yeast extract peptone glycerol (YPG) medium with 3% glycerol was used to confirm petite colonies.

Transporter deletions, revertant strain, and complementation strain construction. The wild-type (WT) strain was *C. glabrata* BG14, which lacked the *ura3* gene. Sequentially multiple deletions were done by using a drug-based recyclable (FRT-NAT1-FRT) cassette, followed by the selection of mutants on the selection plate containing nourseothricin. A homologous recombination-based strategy was used to make deletions as described previously (27). The constructed strains and their respective genotypes are listed in Table S1.

The revertant strain was constructed by the episomal expression of the deleted genes. The modified plasmid pGRB2.3_HphB was made by replacing the *URA3* gene with the *HphB* gene and was then used as the parent plasmid for constructing revertant plasmids. The ABC transporter genes were cloned in plasmid pGRB2.3_HphB under their own promoter by using Gibson assembly. The deletion strains were then transformed with their respective plasmid and confirmed by PCR. Cg*YOR1* complementation in Sc*yor1*Δ was performed by expressing Cg*YOR1* in the expression plasmid pGPD2 under the GAPDH promoter. The plasmid constructs are listed in Table S2.

Drug susceptibility, growth curve, and synergistic assays. The broth microdilution method for detection of MIC, spot dilution assays, and growth kinetics assessments were employed to examine drug susceptibility of these mutants. For this, different classes of antifungals, viz., azoles (fluconazole [FLC], ketoconazole [KTC], voriconazole [VRC], and miconazole [MCZ]), echinocandin (caspofungin [CSF]), polyene (amphotericin B [AmB]), allylamine (terbinafine [TER]), protein synthesis inhibitors (cycloheximide [CHX] and anisomycin [ANY]), DNA damaging agents (4-nitroquinoline, 4-NQO), and metal chelator (1,10-phenanthrolin [OP]) were used.

Susceptibility and synergy to numerous drugs were estimated either by broth microdilution or serial dilution spot assay as described previously (92). The MIC was determined after growing the cells at 30°C in YPD liquid medium for 48 h and taking readings at a wavelength of 600 nm by spectrometer. The MIC$_{80}$ was defined at the lowest concentration inhibiting growth by at least 80% relative to the drug-free YPD control after incubation. For the spot assay, cell suspensions were 10-fold serially diluted in 0.9% saline, and a 3-μL aliquot was spotted on YPD with and without the drug. Agar plates were incubated at 30°C, and growth was recorded after 24 h. All MIC tests and spot tests were undertaken in triplicate. The growth curve assay was undertaken with YPD and using the microcultivation method at 30°C in 96-well plates as described previously (27). The fractional inhibitory concentration index (FICI) was calculated using the following formula: FICI = (MICAcombi/MICAalone) + (MICBcombi/MICBalone). A FICI of ≤0.5 was defined as synergy, a FICI of >0.5 but ≤4.0 was defined as no interaction, and a FICI of >4.0 was defined as antagonism.

For susceptibility profiling under N-limiting conditions, cells were initially grown in complete medium and then transferred into yeast nitrogen base (YNB) medium without amino acid and ammonium sulfate for 12 h. Serial dilutions of the cells were made and spotted on SC complete medium.

R6G efflux and accumulation assay and substrate competition assay. Spectrofluorometric-based R6G efflux was observed as described previously (27). Briefly, yeast strains were cultivated in YPD liquid medium at 200 rpm (30°C) for 16 h, and then secondary culture was grown until mid-log phase. The cells were harvested and washed twice with phosphate-buffered saline (PBS). Cells were suspended in PBS and incubated at 200 rpm (30°C) for 3 h under starvation (glucose free) conditions to reduce ABC pump activity. Cells were then washed twice and diluted to 10^8 cells/mL in PBS. R6G was added at a concentration of 10 μM, and cells were incubated for a further 2 h at 200 rpm (30°C); for the accumulation assay, the supernatants were taken and analyzed with a FACSCalibur flow cytometer (FITC-A filter) using FlowJo v10.3 software. For the efflux assay, 2% glucose was provided as an energy source and incubated for 45 min. After incubation, the supernatants were analyzed with a spectrofluorometer at 527 nm excitation and 555 nm emission. For the substrate competition experiment, the tested substrates BEA, OMY, MYR, GA, FK520, and RAPA, when necessary, were added at a concentration of about 10× MIC along with R6G.

^{3}H-FLC accumulation assay. The ^{3}H-FLC accumulation assay was performed as described previously (93). Overnight-grown (16- h grown culture) samples were washed three times with YNB, starved of glucose for 3 h, and then treated with ^{3}H-FLC in YNB ± 2% glucose in technical triplicate. Samples were incubated with shaking at room temperature for 24 h. At 24 h, the optical density at 600 nm (OD$_{600}$) of each sample was taken, and then a stop solution, consisting of YNB + FLC (20 μM), was mixed with each sample. Then samples were poured over glass microfiber filters on a vacuum and washed again with YNB. Filters with washed cells were placed in scintillation fluid and counted. Values were adjusted to CPM per 10^8 cells based on the OD$_{600}$ of each sample recorded right before filtering. For ^{3}H-FLC efflux measurements, after 24 h, ^{3}H-FLC preloading samples were washed and resuspended in fresh YNB ± 2% glucose, and then intracellular ^{3}H-FLC was measured at the designated time intervals.

Measurement of ROS levels. The oxidant-sensitive probe DCFDA was used to measure endogenous ROS. Cells were set to an OD$_{600}$ of 0.1 in YPD medium and incubated for 4 h at 30°C with shaking at 200 revolutions (rev)/min. Then, DCFDA was added at a final concentration of 2 μM, and the culture was grown for 2 h. The cells were then analyzed with a FACSCalibur flow cytometer at 495 nm excitation and 529 nm emission (FITC-A filter) and analyzed with FlowJo v10.3 software.

Ergosterol measurement and sphingolipidome. Ergosterol was measured by using a UV-spectrometer as described previously (94). Lipid extraction was performed with the Mandala formulation followed by Bligh and Dyer's extraction and base hydrolysis as described earlier (95). Sphingolipids were analyzed by using an LC-MS/MS assay using the QTRAP 4500 (SCIEX, USA) as previously described (82). Data were normalized by ng of sphingolipids/mg of total protein and converted into mole%.

Total RNA isolation and cDNA synthesis and quantitative real-time PCR. Total RNA was extracted by using the RNeasy minikit (Qiagen, Germany). Briefly, overnight-grown cultures of *C. glabrata* were diluted to 0.1 OD_{600} and grown for 4 h at 30°C in YPD. Cells were then washed with PBS, and total RNA was extracted as per the manufacturer's protocol. RNA samples were quantified using a nanodrop 2000 spectrophotometer (Thermo Scientific, USA), and 5 μg of total RNA was used for cDNA synthesis using a RevertAid H minus first-strand cDNA synthesis kit (Thermo Scientific, Lithuania).

The quantitative gene expression profile was evaluated by using a DyNAmo Flash SYBR green qPCR kit (Thermo Scientific, Lithuania) and gene-specific primers, including CgPGK1, for normalization in the CFX96TM real-time PCR system (Bio-Rad, USA). The expression level of the tested genes was measured by comparing the threshold cycle (C_T) value of the gene with CgPGK1. Comparative expression profiles were analyzed with the $2^{-\Delta\Delta CT}$ method. qRT-PCR was performed in biological duplicate with technical triplicate.

Western blot analysis. Western blotting of CgHog1 was performed as described previously (22). Briefly, log-phase-grown *C. glabrata* cells were pelleted down at 5,000 rpm for 10 min and immediately frozen in liquid nitrogen. Cells were lysed using the lysis buffer (50 mM Tris-Cl [pH 7.5]; 1% sodium deoxycholate; 1% Triton X-100; 0.1% SDS; 50 mM sodium fluoride; 0.1 mM sodium vanadate; 5 mM sodium pyrophosphate; 0.05% phenylmethylsulfonyl fluoride [PMSF]; cOmplete EDTA free protease inhibitor cocktail [Roche] 1 tablet per 10 mL). The pelleted cells were lysed in 200 μL of lysis buffer with glass beads by 10 vigorous vortex cycles (1 min vortex with 1 min incubation in ice), and the resulting homogenate was centrifuged at 13,500 $\times$ g for 10 min, and the protein concentration of the supernatant was estimated using Bradford's method. Then, 20 μg protein sample was loaded and resolved by 10% SDS polyacrylamide gel electrophoresis and then blotted onto a nitrocellulose membrane. Phosphorylated CgHog1 protein was detected using anti-dually phosphorylated p38 (α-phospho Hog1) antibody (Cell Signaling Technology), and total CgHog1 protein was detected with anti-Hog1 antibody (Y-215; Santa Cruz Biotechnology). Band intensities were quantified through Image Lab software (Bio-Rad); 0.5 M NaCl was used as osmotic stress to visualize the phosphorylation level of CgHog1. Total CgHog1 was used as a loading control.

Statistical analysis. All analyses were carried out in triplicate forms. Calibration curves were determined using Microsoft Excel. Student's t test was used for statistical significance analysis. Differences of $P < 0.05$ were considered significant.

SUPPLEMENTAL MATERIAL

Supplemental material is available online only.

FIG S1, PPTX file, 0.4 MB.
FIG S2, TIF file, 0.2 MB.
FIG S3, TIF file, 0.2 MB.
FIG S4, TIF file, 0.4 MB.
TABLE S1, DOCX file, 0.02 MB.
TABLE S2, DOCX file, 0.01 MB.
TABLE S3, DOCX file, 0.2 MB.
TABLE S4, DOCX file, 0.02 MB.

REFERENCES

1. Kasper L, Seider K, Hube B. 2015. Intracellular survival of *Candida glabrata* in macrophages: immune evasion and persistence. FEMS Yeast Res 15: fov042. https://doi.org/10.1093/femsyr/fov042.

2. Sheehan DJ, Hitchcock CA, Sibley CM. 1999. Current and emerging azole antifungal agents. Clin Microbiol Rev 12:40–79. https://doi.org/10.1128/CMR.12.1.40.

3. Cowen LE, Sanglard D, Howard SJ, Rogers PD, Perlin DS. 2015. Mechanisms of antifungal drug resistance. Cold Spring Harb Perspect Med 5:a019752. https://doi.org/10.1101/cshperspect.a019752.

4. Fidel PL, Vazquez JA, Sobel JD. 1999. *Candida glabrata*: review of epidemiology, pathogenesis, and clinical disease with comparison to *C. albicans*. Clin Microbiol Rev 12:80–96. https://doi.org/10.1128/CMR.12.1.80.

5. Whaley SG, Zhang Q, Caudle KE, Rogers PD. 2018. Relative contribution of the ABC transporters Cdr1, Pdh1, and Snq2 to azole resistance in *Candida glabrata*. Antimicrob Agents Chemother 62:e01070-18. https://doi.org/10.1128/AAC.01070-18.

6. Healey KR, Zhao Y, Perez WB, Lockhart SR, Sobel JD, Farmakiotis D, Kontoyiannis DP, Sanglard D, Taj-Aldeen SJ, Alexander BD, Jimenez-Ortigosa C, Shor E, Perlin DS. 2016. Prevalent mutator genotype identified in fungal pathogen *Candida glabrata* promotes multi-drug resistance. Nat Commun 7:11128. https://doi.org/10.1038/ncomms11128.

7. Hull CM, Parker JE, Bader O, Weig M, Gross U, Warrilow AGS, Kelly DE, Kelly SL. 2012. Facultative sterol uptake in an ergosterol-deficient clinical isolate of *Candida glabrata* harboring a missense mutation in ERG11 and exhibiting cross-resistance to azoles and amphotericin B. Antimicrob Agents Chemother 56:4223–4232. https://doi.org/10.1128/AAC.06253-11.

8. Teo JQ-M, Lee SJ-Y, Tan A-L, Lim RS-M, Cai Y, Lim T-P, Kwa AL-H. 2019. Molecular mechanisms of azole resistance in Candida bloodstream isolates. BMC Infect Dis 19:63. https://doi.org/10.1186/s12879-019-3672-5.

9. Thakur JK, Arthanari H, Yang F, Pan S-J, Fan X, Breger J, Frueh DP, Gulshan K, Li DK, Mylonakis E, Struhl K, Moye-Rowley WS, Cormack BP, Wagner G, Näär AM. 2008. A nuclear receptor-like pathway regulating multidrug resistance in fungi. Nature 452:604–609. https://doi.org/10.1038/nature06836.

10. Caudle KE, Barker KS, Wiederhold NP, Xu L, Homayouni R, Rogers PD. 2011. Genomewide expression profile analysis of the *Candida glabrata* Pdr1 regulon. Eukaryot Cell 10:373–383. https://doi.org/10.1128/EC.00073-10.

11. Ferrari S, Ischer F, Calabrese D, Posteraro B, Sanguinetti M, Fadda G, Rohde B, Bauser C, Bader O, Sanglard D. 2009. Gain of function mutations in CgPDR1 of *Candida glabrata* not only mediate antifungal resistance but also enhance virulence. PLoS Pathog 5:e1000268. https://doi.org/10.1371/journal.ppat.1000268.

12. Tsai H-F, Krol AA, Sarti KE, Bennett JE. 2006. *Candida glabrata* PDR1, a transcriptional regulator of a pleiotropic drug resistance network, mediates azole resistance in clinical isolates and petite mutants. Antimicrob Agents Chemother 50:1384–1392. https://doi.org/10.1128/AAC.50.4.1384-1392.2006.

13. Sanglard D, Ischer F, Calabrese D, Majcherczyk PA, Bille J. 1999. The ATP binding cassette transporter gene CgCDR1 from *Candida glabrata* is involved in the resistance of clinical isolates to azole antifungal agents. Antimicrob Agents Chemother 43:2753–2765. https://doi.org/10.1128/AAC.43.11.2753.

14. Miyazaki H, Miyazaki Y, Geber A, Parkinson T, Hitchcock C, Falconer DJ, Ward DJ, Marsden K, Bennett JE. 1998. Fluconazole resistance associated with drug efflux and increased transcription of a drug transporter gene, PDH1, in *Candida glabrata*. Antimicrob Agents Chemother 42:1695–1701. https://doi.org/10.1128/AAC.42.7.1695.

15. Sanglard D, Ischer F, Bille J. 2001. Role of ATP-binding-cassette transporter genes in high-frequency acquisition of resistance to azole antifungals in *Candida glabrata*. Antimicrob Agents Chemother 45:1174–1183. https://doi.org/10.1128/AAC.45.4.1174-1183.2001.

16. Sanguinetti M, Posteraro B, Fiori B, Ranno S, Torelli R, Fadda G. 2005. Mechanisms of azole resistance in clinical isolates of *Candida glabrata* collected during a hospital survey of antifungal resistance. Antimicrob Agents Chemother 49:668–679. https://doi.org/10.1128/AAC.49.2.668-679.2005.

17. Torelli R, Posteraro B, Ferrari S, La Sorda M, Fadda G, Sanglard D, Sanguinetti M. 2008. The ATP-binding cassette transporter-encoding gene CgSNQ2 is contributing to the CgPDR1-dependent azole resistance of *Candida glabrata*. Mol Microbiol 68:186–201. https://doi.org/10.1111/j.1365-2958.2008.06143.x.

18. Nagi M, Tanabe K, Ueno K, Nakayama H, Aoyama T, Chibana H, Yamagoe S, Umeyama T, Oura T, Ohno H, Kajiwara S, Miyazaki Y. 2013. The *Candida glabrata* sterol scavenging mechanism, mediated by the ATP-binding cassette transporter Aus1p, is regulated by iron limitation. Mol Microbiol 88:371–381. https://doi.org/10.1111/mmi.12189.

19. Nakayama H, Tanabe K, Bard M, Hodgson W, Wu S, Takemori D, Aoyama T, Kumaraswami NS, Metzler L, Takano Y, Chibana H, Niimi M. 2007. The *Candida glabrata* putative sterol transporter gene CgAUS1 protects cells against azoles in the presence of serum. J Antimicrob Chemother 60:1264–1272. https://doi.org/10.1093/jac/dkm321.

20. Vermitsky J-P, Earhart KD, Smith WL, Homayouni R, Edlind TD, Rogers PD. 2006. Pdr1 regulates multidrug resistance in *Candida glabrata*: gene disruption and genome-wide expression studies. Mol Microbiol 61:704–722. https://doi.org/10.1111/j.1365-2958.2006.05235.x.

21. Ferrari S, Sanguinetti M, De Bernardis F, Torelli R, Posteraro B, Vandeputte P, Sanglard D. 2011. Loss of mitochondrial functions associated with azole resistance in *Candida glabrata* results in enhanced virulence in mice. Antimicrob Agents Chemother 55:1852–1860. https://doi.org/10.1128/AAC.01271-10.

22. Khandelwal NK, Chauhan N, Sarkar P, Esquivel BD, Coccetti P, Singh A, Coste AT, Gupta M, Sanglard D, White TC, Chauvel M, d'Enfert C, Chattopadhyay A, Gaur NA, Mondal AK, Prasad R. 2018. Azole resistance in a *Candida albicans* mutant lacking the ABC transporter CDR6/ROA1 depends on TOR signaling. J Biol Chem 293:412–432. https://doi.org/10.1074/jbc.M117.807032.

23. Robbins N, Collins C, Morhayim J, Cowen LE. 2010. Metabolic control of antifungal drug resistance. Fungal Genet Biol 47:81–93. https://doi.org/10.1016/j.fgb.2009.07.004.

24. Singh-Babak SD, Babak T, Diezmann S, Hill JA, Xie JL, Chen Y-L, Poutanen SM, Rennie RP, Heitman J, Cowen LE. 2012. Global analysis of the evolution and mechanism of echinocandin resistance in *Candida glabrata*. PLoS Pathog 8:e1002718. https://doi.org/10.1371/journal.ppat.1002718.

25. Kumari S, Kumar M, Khandelwal NK, Kumari P, Varma M, Vishwakarma P, Shahi G, Sharma S, Lynn AM, Prasad R, Gaur NA. 2018. ABC transportome inventory of human pathogenic yeast *Candida glabrata*: phylogenetic and expression analysis. PLoS One 13:e0202993. https://doi.org/10.1371/journal.pone.0202993.

26. Borah S, Shivarathri R, Kaur R. 2011. The Rho1 GTPase-activating protein CgBem2 is required for survival of azole stress in *Candida glabrata*. J Biol Chem 286:34311–34324. https://doi.org/10.1074/jbc.M111.264671.

27. Kumari S, Kumar M, Khandelwal NK, Pandey AK, Bhakt P, Kaur R, Prasad R, Gaur NA. 2020. A homologous overexpression system to study roles of drug transporters in *Candida glabrata*. FEMS Yeast Res 20:foaa032. https://doi.org/10.1093/femsyr/foaa032.

28. Decottignies A, Lambert L, Catty P, Degand H, Epping EA, Moye-Rowley WS, Balzi E, Goffeau A. 1995. Identification and characterization of SNQ2, a new multidrug ATP binding cassette transporter of the yeast plasma membrane. J Biol Chem 270:18150–18157. https://doi.org/10.1074/jbc.270.30.18150.

29. Servos J, Haase E, Brendel M. 1993. Gene SNQ2 of *Saccharomyces cerevisiae*, which confers resistance to 4-nitroquinoline-N-oxide and other chemicals, encodes a 169 kDa protein homologous to ATP-dependent permeases. Mol Gen Genet 236:214–218. https://doi.org/10.1007/BF00277115.

30. Kolaczkowska A, Kolaczkowski M, Goffeau A, Moye-Rowley WS. 2008. Compensatory activation of the multidrug transporters Pdr5p, Snq2p, and Yor1p by Pdr1p in *Saccharomyces cerevisiae*. FEBS Lett 582:977–983. https://doi.org/10.1016/j.febslet.2008.02.045.

31. Kolaczkowski M, Kolaczkowska A, Luczynski J, Witek S, Goffeau A. 1998. In vivo characterization of the drug resistance profile of the major ABC transporters and other components of the yeast pleiotropic drug resistance network. Microb Drug Resist 4:143–158. https://doi.org/10.1089/mdr.1998.4.143.

32. Katzmann DJ, Hallstrom TC, Voet M, Wysock W, Golin J, Volckaert G, Moye-Rowley WS. 1995. Expression of an ATP-binding cassette transporter-encoding gene (YOR1) is required for oligomycin resistance in *Saccharomyces cerevisiae*. Mol Cell Biol 15:6875–6883. https://doi.org/10.1128/MCB.15.12.6875.

33. Ramírez-Zavala B, Manz H, Englert F, Rogers PD, Morschhäuser J. 2018. A hyperactive form of the zinc cluster transcription factor Stb5 causes YOR1 overexpression and beauvericin resistance in *Candida albicans*. Antimicrob Agents Chemother 62:e01655-18. https://doi.org/10.1128/AAC.01655-18.

34. Shekhar-Guturja T, Gunaherath GMKB, Wijeratne EMK, Lambert J-P, Averette AF, Lee SC, Kim T, Bahn Y-S, Tripodi F, Ammar R, Döhl K, Niewola-Staszkowska K, Schmitt L, Loewith RJ, Roth FP, Sanglard D, Andes D, Nislow C, Coccetti P, Gingras A-C, Heitman J, Gunatilaka AAL, Cowen LE. 2016. Dual action antifungal small molecule modulates multidrug efflux and TOR signaling. Nat Chem Biol 12:867–875. https://doi.org/10.1038/nchembio.2165.

35. Shekhar-Guturja T, Tebung WA, Mount H, Liu N, Köhler JR, Whiteway M, Cowen LE. 2016. Beauvericin potentiates azole activity via inhibition of multidrug efflux, blocks *Candida albicans* morphogenesis, and is effluxed via Yor1 and circuitry controlled by Zcf29. Antimicrob Agents Chemother 60:7468–7480. https://doi.org/10.1128/AAC.01959-16.

36. Mansfield BE, Oltean HN, Oliver BG, Hoot SJ, Leyde SE, Hedstrom L, White TC. 2010. Azole drugs are imported by facilitated diffusion in Candida

albicans and other pathogenic fungi. PLoS Pathog 6:e1001126. https://doi.org/10.1371/journal.ppat.1001126.

37. Li QQ, Tsai H-F, Mandal A, Walker BA, Noble JA, Fukuda Y, Bennett JE. 2018. Sterol uptake and sterol biosynthesis act coordinately to mediate antifungal resistance in Candida glabrata under azole and hypoxic stress. Mol Med Rep 17:6585–6597. https://doi.org/10.3892/mmr.2018.8716.

38. Miyazaki T, Kohno S. 2014. ER stress response mechanisms in the pathogenic yeast Candida glabrata and their roles in virulence. Virulence 5:365–370. https://doi.org/10.4161/viru.27373.

39. Chaillot J, Tebbji F, Remmal A, Boone C, Brown GW, Bellaoui M, Sellam A. 2015. The monoterpene carvacrol generates endoplasmic reticulum stress in the pathogenic fungus Candida albicans. Antimicrob Agents Chemother 59:4584–4592. https://doi.org/10.1128/AAC.00551-15.

40. Delattin N, Cammue BP, Thevissen K. 2014. Reactive oxygen species-inducing antifungal agents and their activity against fungal biofilms. Future Med Chem 6:77–90. https://doi.org/10.4155/fmc.13.189.

41. Mahl CD, Behling CS, Hackenhaar FS, de Carvalho e Silva MN, Putti J, Salomon TB, Alves SH, Fuentefria A, Benfato MS. 2015. Induction of ROS generation by fluconazole in Candida glabrata: activation of antioxidant enzymes and oxidative DNA damage. Diagn Microbiol Infect Dis 82:203–208. https://doi.org/10.1016/j.diagmicrobio.2015.03.019.

42. Peng CA, Gaertner AAE, Henriquez SA, Fang D, Colon-Reyes RJ, Brumaghim JL, Kozubowski L. 2018. Fluconazole induces ROS in Cryptococcus neoformans and contributes to DNA damage in vitro. PLoS One 13:e0208471. https://doi.org/10.1371/journal.pone.0208471.

43. Austriaco N. 2012. Endoplasmic reticulum involvement in yeast cell death. Front Oncol 2:87. https://doi.org/10.3389/fonc.2012.00087.

44. Hernández-Elvira M, Martínez-Gómez R, Domínguez-Martin E, Méndez A, Kawasaki L, Ongay-Larios L, Coria R. 2019. Tunicamycin sensitivity-suppression by high gene dosage reveals new functions of the yeast Hog1 MAP Kinase. Cells 8:710. https://doi.org/10.3390/cells8070710.

45. Rastogi RP, Singh SP, Häder D-P, Sinha RP. 2010. Detection of reactive oxygen species (ROS) by the oxidant-sensing probe 2′,7′-dichlorodihydrofluorescein diacetate in the cyanobacterium Anabaena variabilis PCC 7937. Biochem Biophys Res Commun 397:603–607. https://doi.org/10.1016/j.bbrc.2010.06.006.

46. Otsubo Y, Nakashima A, Yamamoto M, Yamashita A. 2017. TORC1-dependent phosphorylation targets in fission yeast. Biomolecules 7:50. https://doi.org/10.3390/biom7030050.

47. Murai T, Nakase Y, Fukuda K, Chikashige Y, Tsutsumi C, Hiraoka Y, Matsumoto T. 2009. Distinctive responses to nitrogen starvation in the dominant active mutants of the fission yeast Rheb GTPase. Genetics 183:517–527. https://doi.org/10.1534/genetics.109.105379.

48. Tesnière C, Pradal M, Bessière C, Sanchez I, Blondin B, Bigey F. 2018. Relief from nitrogen starvation triggers transient destabilization of glycolytic mRNAs in Saccharomyces cerevisiae cells. Mol Biol Cell 29:490–498. https://doi.org/10.1091/mbc.E17-01-0061.

49. Wedaman KP, Reinke A, Anderson S, Yates J, McCaffery JM, Powers T. 2003. Tor kinases are in distinct membrane-associated protein complexes in Saccharomyces cerevisiae. Mol Biol Cell 14:1204–1220. https://doi.org/10.1091/mbc.e02-09-0609.

50. Jandric Z, Gregori C, Klopf E, Radolf M, Schüller C. 2013. Sorbic acid stress activates the Candida glabrata high osmolarity glycerol MAP kinase pathway. Front Microbiol 4:350. https://doi.org/10.3389/fmicb.2013.00350.

51. Shertz CA, Bastidas RJ, Li W, Heitman J, Cardenas ME. 2010. Conservation, duplication, and loss of the Tor signaling pathway in the fungal kingdom. BMC Genomics 11:510. https://doi.org/10.1186/1471-2164-11-510.

52. Shimobayashi M, Oppliger W, Moes S, Jenö P, Hall MN. 2013. TORC1-regulated protein kinase Npr1 phosphorylates Orm to stimulate complex sphingolipid synthesis. Mol Biol Cell 24:870–881. https://doi.org/10.1091/mbc.E12-10-0753.

53. Loewith R, Hall MN. 2011. Target of rapamycin (TOR) in nutrient signaling and growth control. Genetics 189:1177–1201. https://doi.org/10.1534/genetics.111.133363.

54. Beck T, Hall MN. 1999. The TOR signalling pathway controls nuclear localization of nutrient-regulated transcription factors. Nature 402:689–692. https://doi.org/10.1038/45287.

55. Liao H-C, Chen M-Y. 2012. Target of rapamycin complex 2 signals to downstream effector yeast protein kinase 2 (Ypk2) through adheres-voraciously-to-target-of-rapamycin-2 protein 1 (Avo1) in Saccharomyces cerevisiae. J Biol Chem 287:6089–6099. https://doi.org/10.1074/jbc.M111.303701.

56. Montefusco DJ, Matmati N, Hannun YA. 2014. The yeast sphingolipid signaling landscape. Chem Phys Lipids 177:26–40. https://doi.org/10.1016/j.chemphyslip.2013.10.006.

57. Song J, Liu X, Li R. 2020. Sphingolipids: regulators of azole drug resistance and fungal pathogenicity. Mol Microbiol 114:891–905. https://doi.org/10.1111/mmi.14586.

58. Aronova S, Wedaman K, Aronov PA, Fontes K, Ramos K, Hammock BD, Powers T. 2008. Regulation of ceramide biosynthesis by TOR complex 2. Cell Metab 7:148–158. https://doi.org/10.1016/j.cmet.2007.11.015.

59. Miyazaki T, Yamauchi S, Inamine T, Nagayoshi Y, Saijo T, Izumikawa K, Seki M, Kakeya H, Yamamoto Y, Yanagihara K, Miyazaki Y, Kohno S. 2010. Roles of calcineurin and Crz1 in antifungal susceptibility and virulence of Candida glabrata. Antimicrob Agents Chemother 54:1639–1643. https://doi.org/10.1128/AAC.01364-09.

60. Steinbach WJ, Reedy JL, Cramer RA, Perfect JR, Heitman J. 2007. Harnessing calcineurin as a novel anti-infective agent against invasive fungal infections. Nat Rev Microbiol 5:418–430. https://doi.org/10.1038/nrmicro1680.

61. Sanchez-Casalongue ME, Lee J, Diamond A, Shuldiner S, Moir RD, Willis IM. 2015. Differential phosphorylation of a regulatory subunit of protein kinase CK2 by target of rapamycin complex 1 signaling and the Cdc-like kinase Kns1. J Biol Chem 290:7221–7233. https://doi.org/10.1074/jbc.M114.626523.

62. Alaalm L, Crunden JL, Butcher M, Obst U, Whealy R, Williamson CE, O'Brien HE, Schaffitzel C, Ramage G, Diezmann S. 2020. A novel Hsp90 phospho-switch modulates virulence in the major human fungal pathogen Candida albicans. bioRxiv https://doi.org/10.1101/2020.09.23.309831.

63. Shapiro RS, Robbins N, Cowen LE. 2011. Regulatory circuitry governing fungal development, drug resistance, and disease. Microbiol Mol Biol Rev 75:213–267. https://doi.org/10.1128/MMBR.00045-10.

64. Bruno VM, Mitchell AP. 2005. Regulation of azole drug susceptibility by Candida albicans protein kinase CK2. Mol Microbiol 56:559–573. https://doi.org/10.1111/j.1365-2958.2005.04562.x.

65. Cowen LE, Lindquist S. 2005. Hsp90 potentiates the rapid evolution of new traits: drug resistance in diverse fungi. Science 309:2185–2189. https://doi.org/10.1126/science.1118370.

66. Cowen LE, Carpenter AE, Matangkasombut O, Fink GR, Lindquist S. 2006. Genetic architecture of Hsp90-dependent drug resistance. Eukaryot Cell 5:2184–2188. https://doi.org/10.1128/EC.00274-06.

67. Diezmann S, Michaut M, Shapiro RS, Bader GD, Cowen LE. 2012. Mapping the Hsp90 genetic interaction network in Candida albicans reveals environmental contingency and rewired circuitry. PLoS Genet 8:e1002562. https://doi.org/10.1371/journal.pgen.1002562.

68. Prasad R, Khandelwal NK, Banerjee A. 2016. Yeast ABC transporters in lipid trafficking. Fungal Genet Biol 93:25–34. https://doi.org/10.1016/j.fgb.2016.05.008.

69. Rizzo J, Stanchev LD, da Silva VKA, Nimrichter L, Pomorski TG, Rodrigues ML. 2019. Role of lipid transporters in fungal physiology and pathogenicity. Comput Struct Biotechnol J 17:1278–1289. https://doi.org/10.1016/j.csbj.2019.09.001.

70. Decottignies A, Grant AM, Nichols JW, de Wet H, McIntosh DB, Goffeau A. 1998. ATPase and multidrug transport activities of the overexpressed yeast ABC protein Yor1p. J Biol Chem 273:12612–12622. https://doi.org/10.1074/jbc.273.20.12612.

71. Jungwirth H, Kuchler K. 2006. Yeast ABC transporters: a tale of sex, stress, drugs and aging. FEBS Lett 580:1131–1138. https://doi.org/10.1016/j.febslet.2005.12.050.

72. Khandelwal NK, Kaemmer P, Förster TM, Singh A, Coste AT, Andes DR, Hube B, Sanglard D, Chauhan N, Kaur R, d'Enfert C, Mondal AK, Prasad R. 2016. Pleiotropic effects of the vacuolar ABC transporter MLT1 of Candida albicans on cell function and virulence. Biochem J 473:1537–1552. https://doi.org/10.1042/BCJ20160024.

73. Paumi CM, Chuk M, Snider J, Stagljar I, Michaelis S. 2009. ABC transporters in Saccharomyces cerevisiae and their interactors: new technology advances the biology of the ABCC (MRP) subfamily. Microbiol Mol Biol Rev 73:577–593. https://doi.org/10.1128/MMBR.00020-09.

74. Orsi CF, Colombari B, Ardizzoni A, Peppoloni S, Neglia R, Posteraro B, Morace G, Fadda G, Blasi E. 2009. The ABC transporter-encoding gene AFR1 affects the resistance of Cryptococcus neoformans to microglia-mediated antifungal activity by delaying phagosomal maturation. FEMS Yeast Res 9:301–310. https://doi.org/10.1111/j.1567-1364.2008.00470.x.

75. Paul S, Diekema D, Moye-Rowley WS. 2013. Contributions of Aspergillus fumigatus ATP-binding cassette transporter proteins to drug resistance and virulence. Eukaryot Cell 12:1619–1628. https://doi.org/10.1128/EC.00171-13.

76. Chaturvedi V, Springer DJ, Behr MJ, Ramani R, Li X, Peck MK, Ren P, Bopp DJ, Wood B, Samsonoff WA, Butchkoski CM, Hicks AC, Stone WB, Rudd RJ, Chaturvedi S. 2010. Morphological and molecular characterizations of

psychrophilic fungus *Geomyces destructans* from New York bats with white nose syndrome (WNS). PLoS One 5:e10783. https://doi.org/10.1371/journal.pone.0010783.

77. Fonseca E, Silva S, Rodrigues CF, Alves CT, Azeredo J, Henriques M. 2014. Effects of fluconazole on *Candida glabrata* biofilms and its relationship with ABC transporter gene expression. Biofouling 30:447–457. https://doi.org/10.1080/08927014.2014.886108.

78. Jiang L, Xu D, Chen Z, Cao Y, Gao P, Jiang Y. 2016. The putative ABC transporter encoded by the orf19.4531 plays a role in the sensitivity of *Candida albicans* cells to azole antifungal drugs. FEMS Yeast Res 16:fow024. https://doi.org/10.1093/femsyr/fow024.

79. Kean R, Delaney C, Sherry L, Borman A, Johnson EM, Richardson MD, Rautemaa-Richardson R, Williams C, Ramage G. 2018. Transcriptome assembly and profiling of *Candida auris* reveals novel insights into biofilm-mediated resistance. mSphere 3:e00334-18. https://doi.org/10.1128/mSphere.00334-18.

80. Klug L, Daum G. 2014. Yeast lipid metabolism at a glance. FEMS Yeast Res 14:369–388. https://doi.org/10.1111/1567-1364.12141.

81. Gao J, Wang H, Li Z, Wong AH-H, Wang Y-Z, Guo Y, Lin X, Zeng G, Liu H, Wang Y, Wang J. 2018. *Candida albicans* gains azole resistance by altering sphingolipid composition. Nat Commun 9:1–14. https://doi.org/10.1038/s41467-018-06944-1.

82. Kumar M, Singh A, Kumari S, Kumar P, Wasi M, Mondal AK, Rudramurthy SM, Chakrabarti A, Gaur NA, Gow NAR, Prasad R. 2021. Sphingolipidomics of drug resistant *Candida auris* clinical isolates reveal distinct sphingolipid species signatures. Biochim Biophys Acta Mol Cell Biol Lipids 1866:158815. https://doi.org/10.1016/j.bbalip.2020.158815.

83. Zhai P, Song J, Gao L, Lu L. 2019. A sphingolipid synthesis-related protein OrmA in *Aspergillus fumigatus* is responsible for azole susceptibility and virulence. Cell Microbiol 21:e13092. https://doi.org/10.1111/cmi.13092.

84. Panwar SL, Moye-Rowley WS. 2006. Long chain base tolerance in *Saccharomyces cerevisiae* is induced by retrograde signals from the mitochondria. J Biol Chem 281:6376–6384. https://doi.org/10.1074/jbc.M512115200.

85. Vandenbosch D, Bink A, Govaert G, Cammue BPA, Nelis HJ, Thevissen K, Coenye T. 2012. Phytosphingosine-1-phosphate is a signaling molecule involved in miconazole resistance in sessile *Candida albicans* cells. Antimicrob Agents Chemother 56:2290–2294. https://doi.org/10.1128/AAC.05106-11.

86. Matmati N, Metelli A, Tripathi K, Yan S, Mohanty BK, Hannun YA. 2013. Identification of C18:1-phytoceramide as the candidate lipid mediator for hydroxyurea resistance in yeast. J Biol Chem 288:17272–17284. https://doi.org/10.1074/jbc.M112.444802.

87. LaFayette SL, Collins C, Zaas AK, Schell WA, Betancourt-Quiroz M, Gunatilaka AAL, Perfect JR, Cowen LE. 2010. PKC signaling regulates drug resistance of the fungal pathogen *Candida albicans* via circuitry comprised of Mkc1, calcineurin, and Hsp90. PLoS Pathog 6:e1001069. https://doi.org/10.1371/journal.ppat.1001069.

88. Singh SD, Robbins N, Zaas AK, Schell WA, Perfect JR, Cowen LE. 2009. Hsp90 governs echinocandin resistance in the pathogenic yeast *Candida albicans* via calcineurin. PLoS Pathog 5:e1000532. https://doi.org/10.1371/journal.ppat.1000532.

89. Blankenship JR, Wormley FL, Boyce MK, Schell WA, Filler SG, Perfect JR, Heitman J. 2003. Calcineurin is essential for *Candida albicans* survival in serum and virulence. Eukaryot Cell 2:422–430. https://doi.org/10.1128/EC.2.3.422-430.2003.

90. Chen Y-L, Brand A, Morrison EL, Silao FGS, Bigol UG, Malbas FF, Nett JE, Andes DR, Solis NV, Filler SG, Averette A, Heitman J. 2011. Calcineurin controls drug tolerance, hyphal growth, and virulence in *Candida dubliniensis*. Eukaryot Cell 10:803–819. https://doi.org/10.1128/EC.00310-10.

91. Sanglard D, Ischer F, Marchetti O, Entenza J, Bille J. 2003. Calcineurin A of *Candida albicans*: involvement in antifungal tolerance, cell morphogenesis and virulence. Mol Microbiol 48:959–976. https://doi.org/10.1046/j.1365-2958.2003.03495.x.

92. Wind CM, de Vries HJC, van Dam AP. 2015. Determination of in vitro synergy for dual antimicrobial therapy against resistant *Neisseria gonorrhoeae* using Etest and agar dilution. Int J Antimicrob Agents 45:305–308. https://doi.org/10.1016/j.ijantimicag.2014.10.020.

93. Rybak JM, Muñoz JF, Barker KS, Parker JE, Esquivel BD, Berkow EL, Lockhart SR, Gade L, Palmer GE, White TC, Kelly SL, Cuomo CA, Rogers PD. 2020. Mutations in TAC1B: a novel genetic determinant of clinical fluconazole resistance in *Candida auris*. mBio 11:e00365-20. https://doi.org/10.1128/mBio.00365-20.

94. Arthington-Skaggs BA, Jradi H, Desai T, Morrison CJ. 1999. Quantitation of ergosterol content: novel method for determination of fluconazole susceptibility of *Candida albicans*. J Clin Microbiol 37:3332–3337. https://doi.org/10.1128/JCM.37.10.3332-3337.1999.

95. Singh A, MacKenzie A, Girnun G, Del Poeta M. 2017. Analysis of sphingolipids, sterols, and phospholipids in human pathogenic *Cryptococcus* strains. J Lipid Res 58:2017–2036.]. https://doi.org/10.1194/jlr.M078600.